513th Euromech Colloquium on "Dynamics of non-spherical particles in fluid turbulence"
Udine, Italy, April 6-8, 2011

Deformable Fibers and non-spherical particles in suspension flow

Cyrus K Aidun

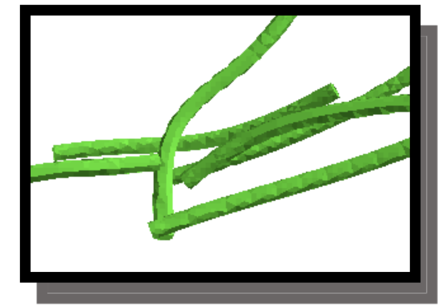

Students: Brian Yun and Daniel Reasor
Former students: Hanjiang Xu, Jon Clausen
Former Postdoc: E-Jiang Deng, Mehran Parsheh

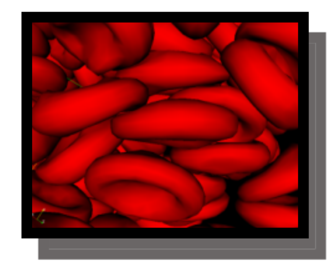

Georgia Tech **George W. Woodruff School of Mechanical Engineering**

NSF TeraGrid **NSF TeraGrid TG-CTS100012**

OUTLINE

- Effect of fiber deformation and orientation distribution on suspension rheology
  - Fiber suspension in turbulent channel flow
  - Deformation characterization in shear flow: rheology
- Lagrangian turbulence with deformable particles (red blood cells) and particle migration…

Experiment Setup

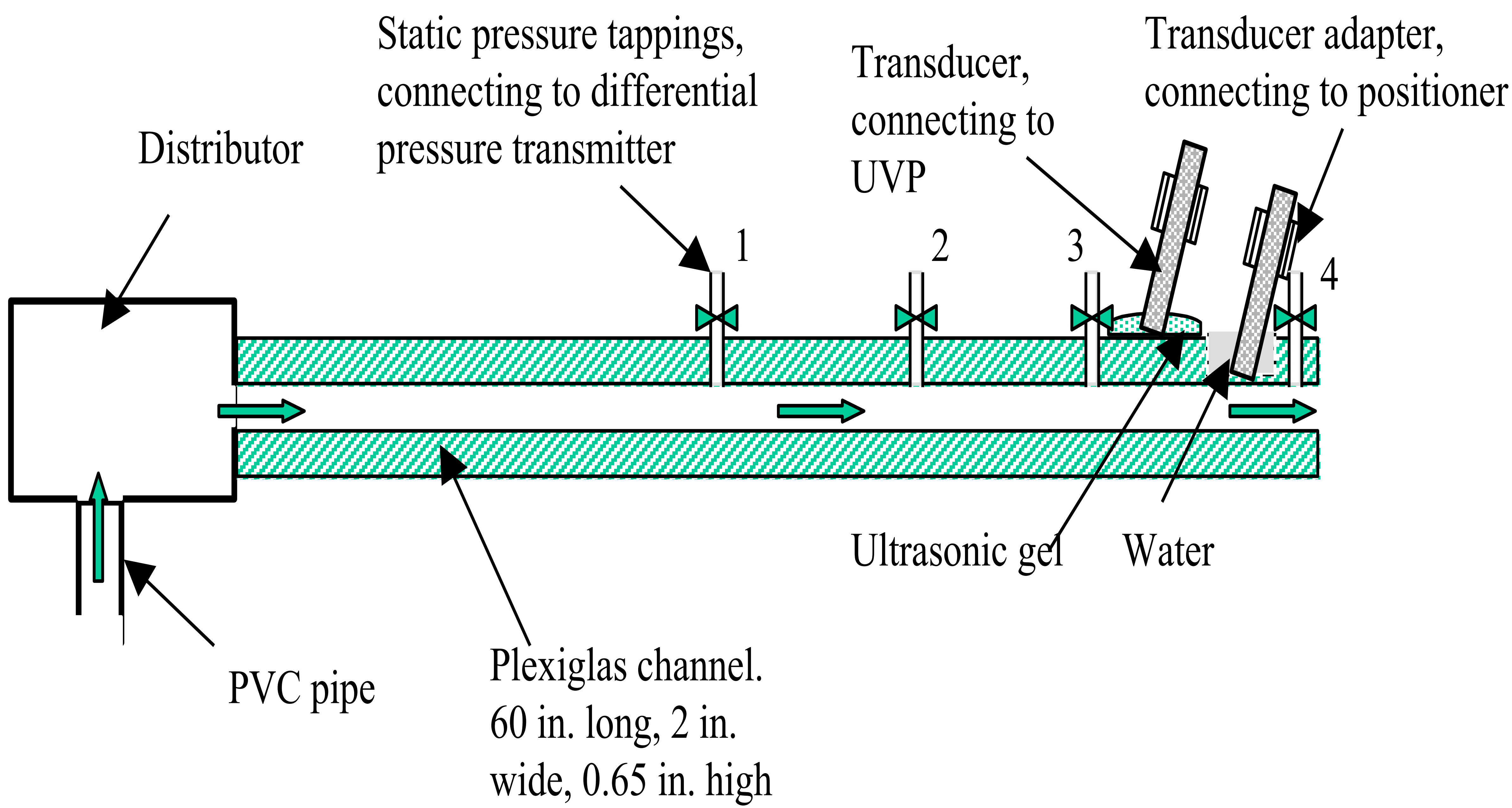

Xu, H., and Aidun, C.K., "Characteristics of Fiber Suspension Flow in a Rectangular Channel" *Int. J. Multiphase Flow*, 3 1/3, pp. 318-336, 2005

Basic Principle of PUDV

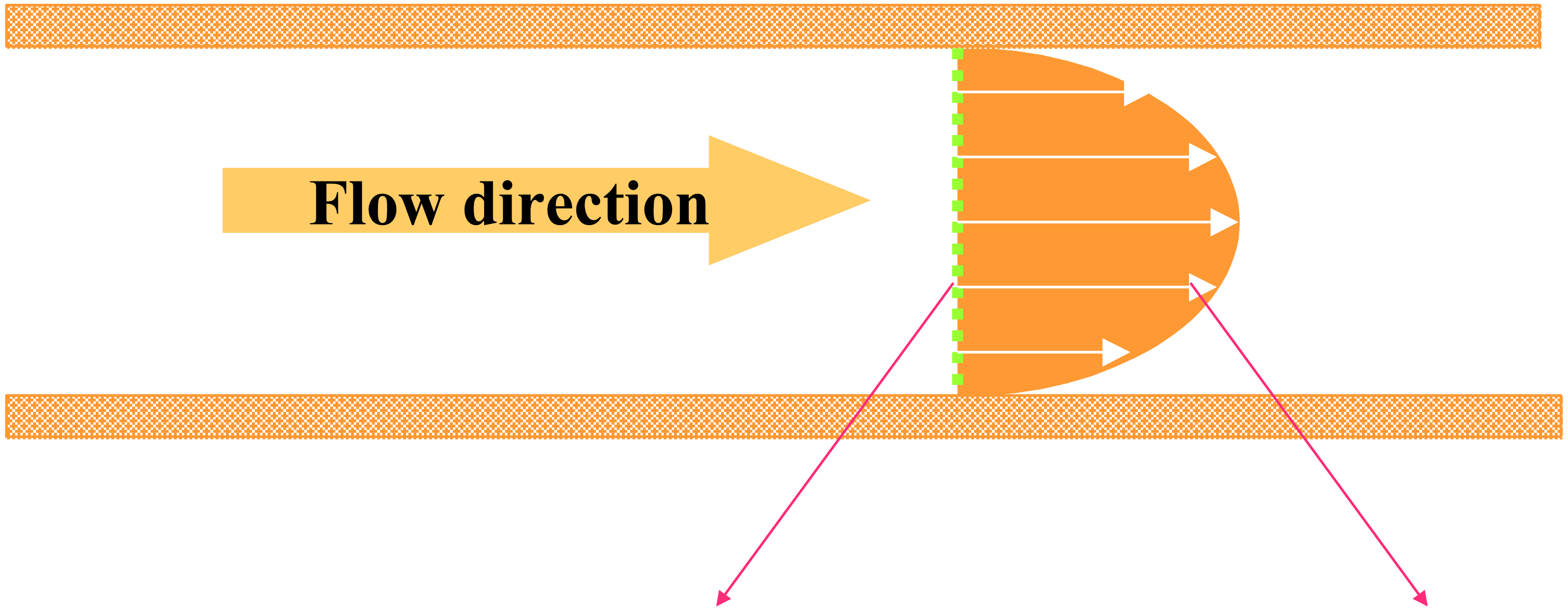

Two parameters: **(1) Location** **(2) Velocity at the measuring point**

Basic Principle of PUDV

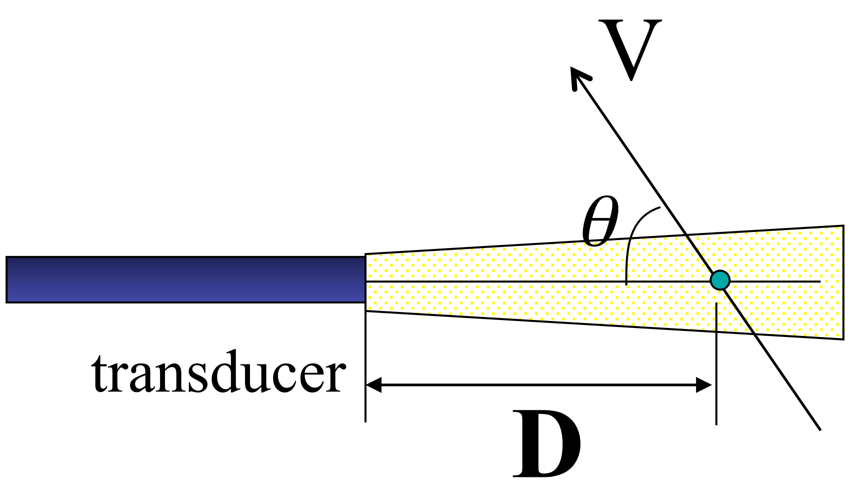

(1) Doppler effect:

$$f_d = \pm \frac{2V\cos\theta}{c} f_e$$

(2) Echography

$$D = \frac{c \cdot t}{2}$$

f_d : Frequency shift

V: Particle speed

θ: Angle between ultrasound and particle direction

f_e: Frequency of Ultrasound

c: Speed of ultrasound

D: Distance between particle and transducer

t: Time between signal transmission and reception

Internal architecture and measuring principle of PUDV

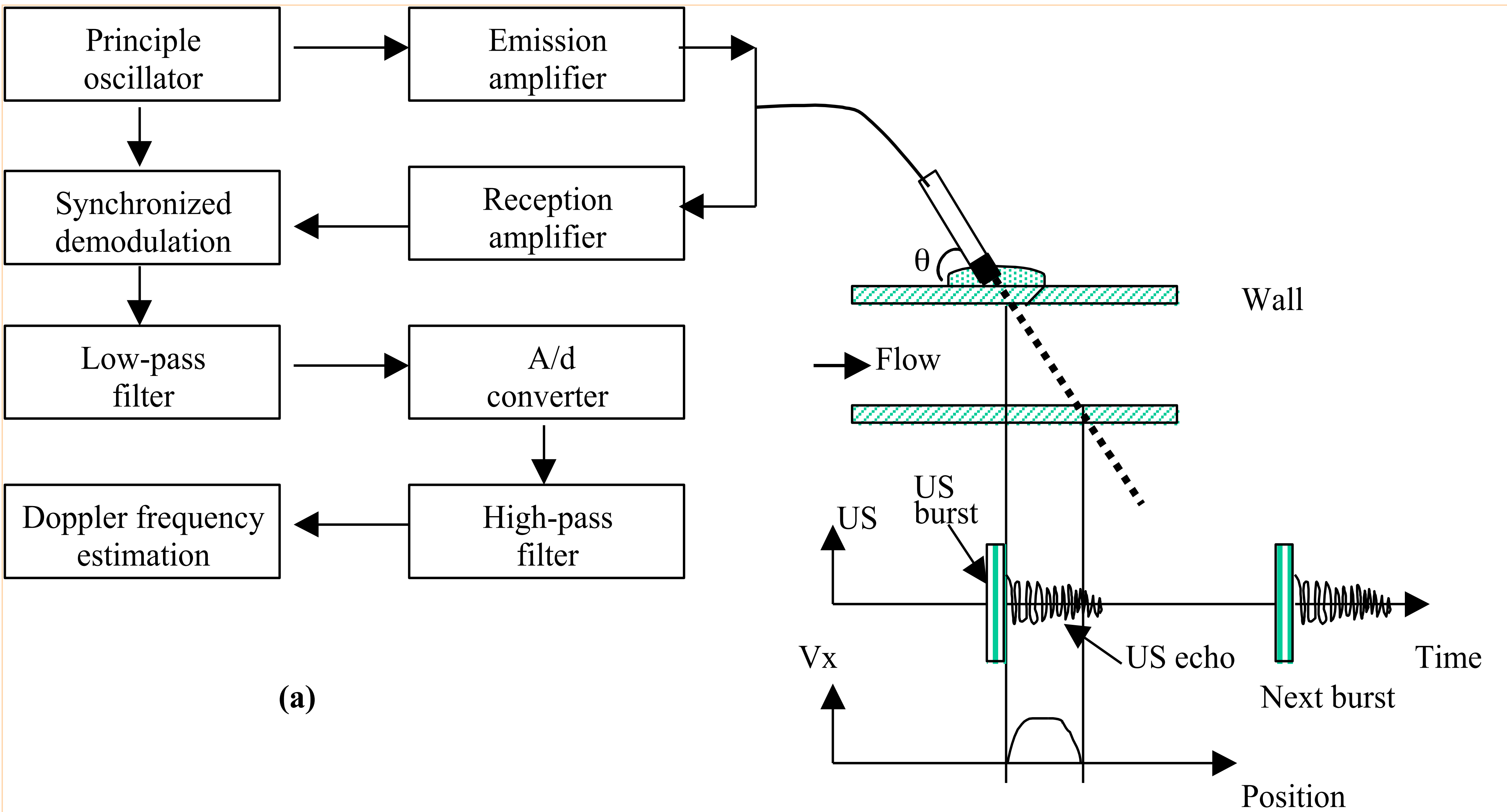

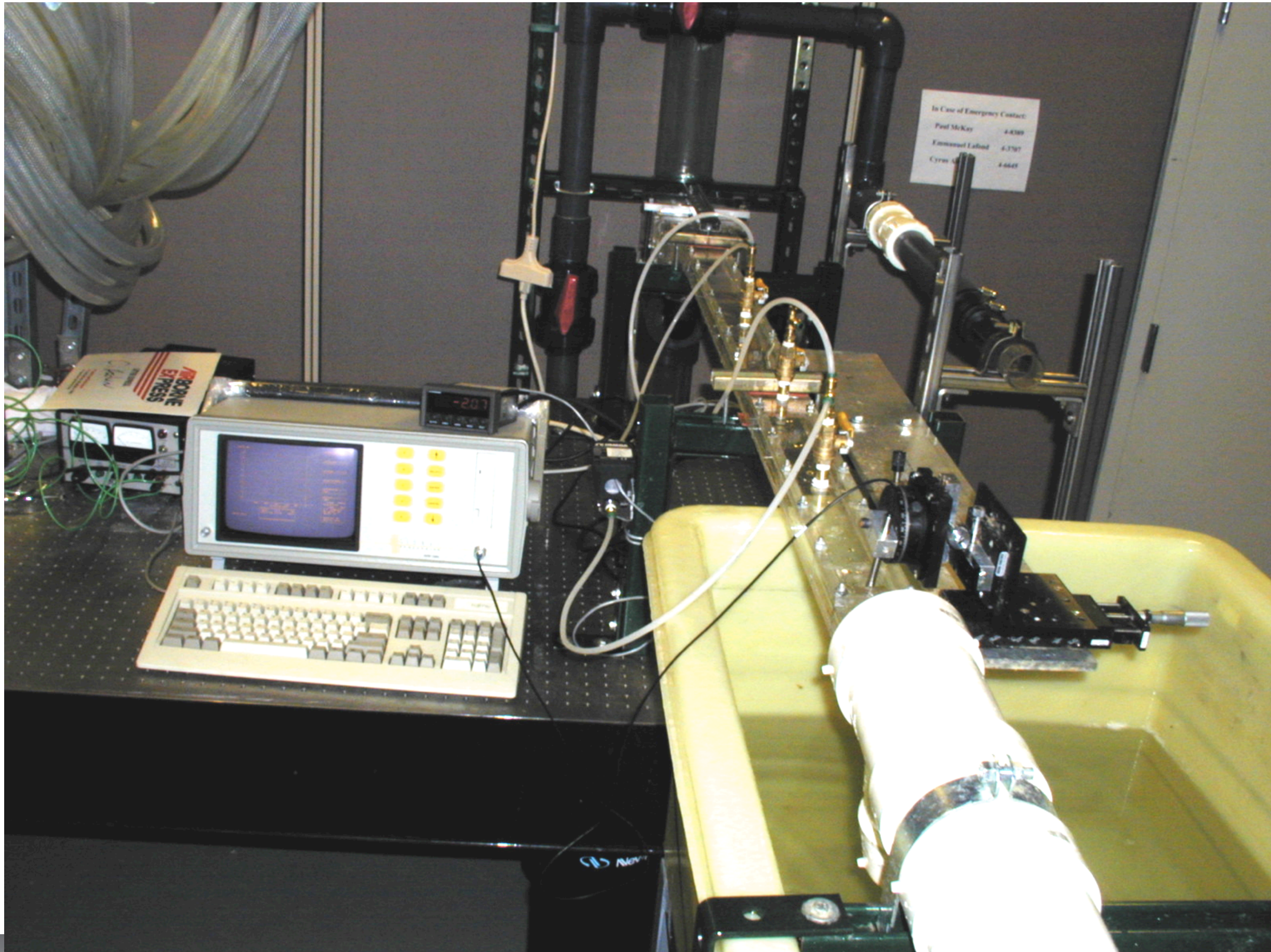
In Case of Emergency Contact:
Paul McKay
AIRBORNE EXPRESS

Sensitivity of PUDV measurement of fiber suspension

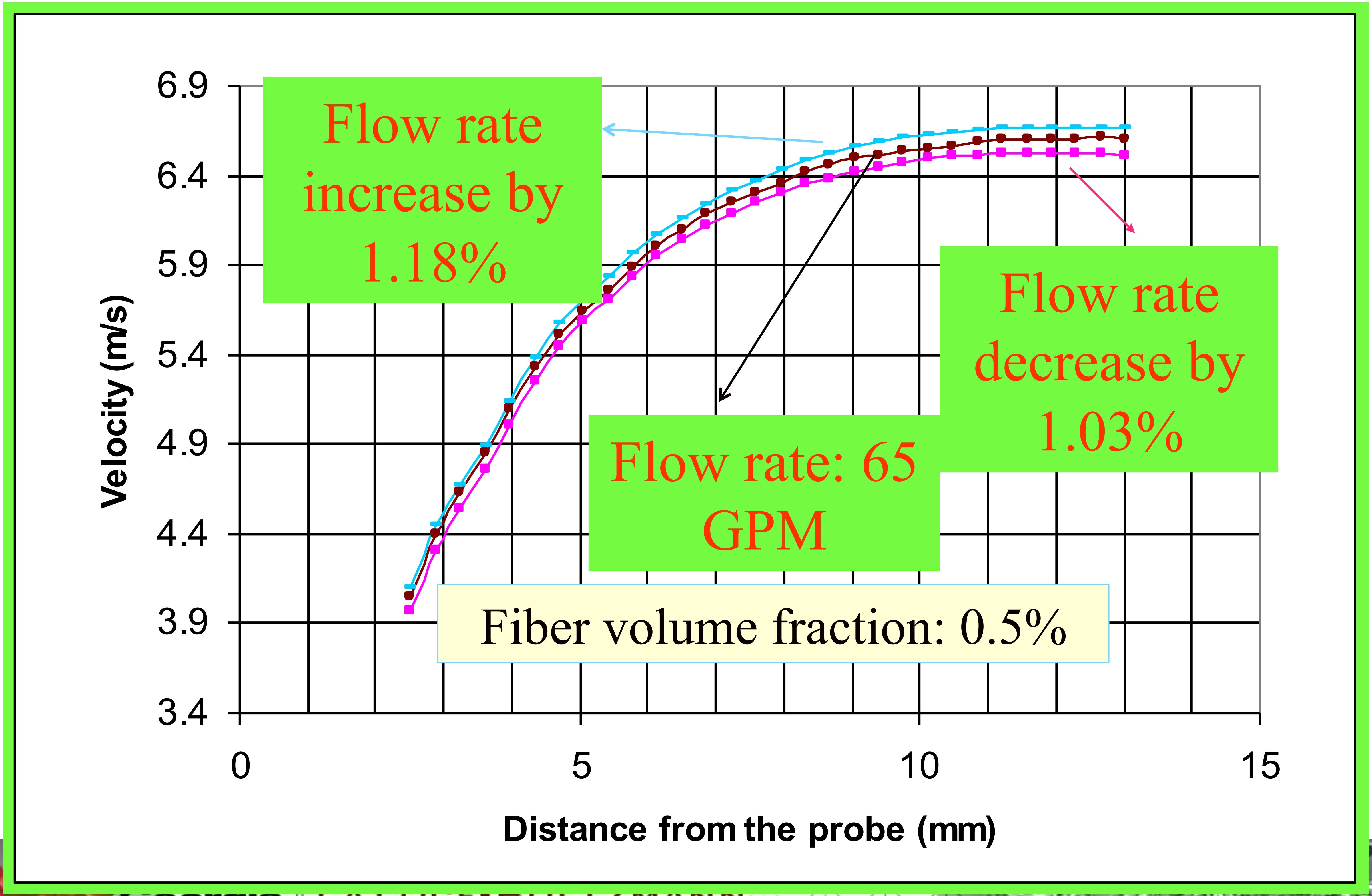

Characterizations of fiber suspension flow

Flow rate (Gal/minute)	Uavg (m/s)	Re	Volume concentration (%)						
			0.05	0.1	0.15	0.3	0.5	0.75	1.0
2.2	0.157	2050		✓	✓	✓	✓	✓	
3.3	0.231	3025		✓	✓	✓	✓	✓	✓
6.5	0.454	5940		✓	✓	✓	✓	✓	✓
13	0.908	11880	✓	✓	✓	✓	✓	✓	✓
40	2.90	36625	✓	✓	✓	✓	✓	✓	✓
65	4.56	59638	✓	✓	✓	✓	✓	✓	✓
80	5.60	73250	✓	✓	✓	✓	✓	✓	✓
100	7.0	91510	✓	✓	✓	✓	✓	✓	✓

Velocity profile of water measured by PUDV at different flow rate

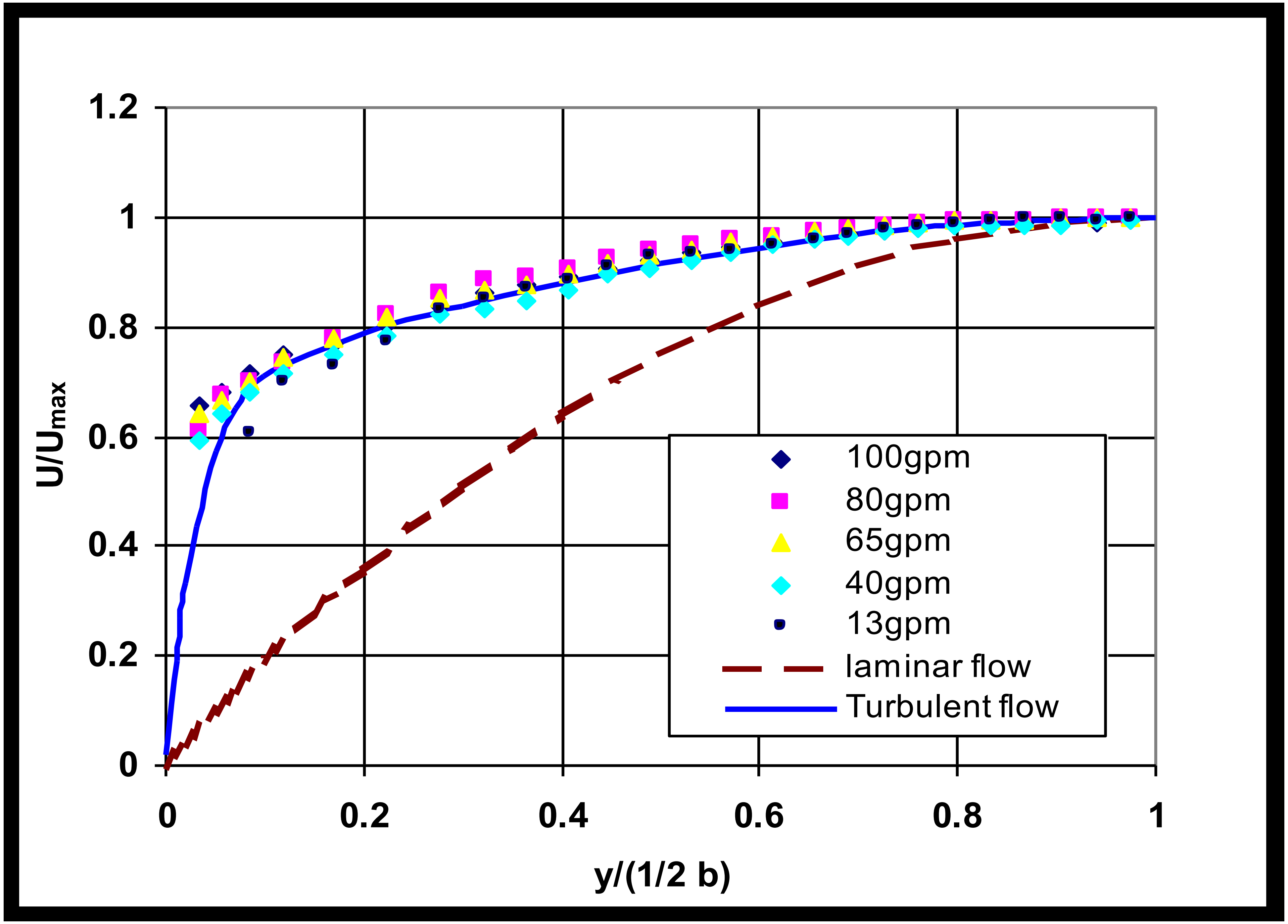

Effect of concentration on velocity profile

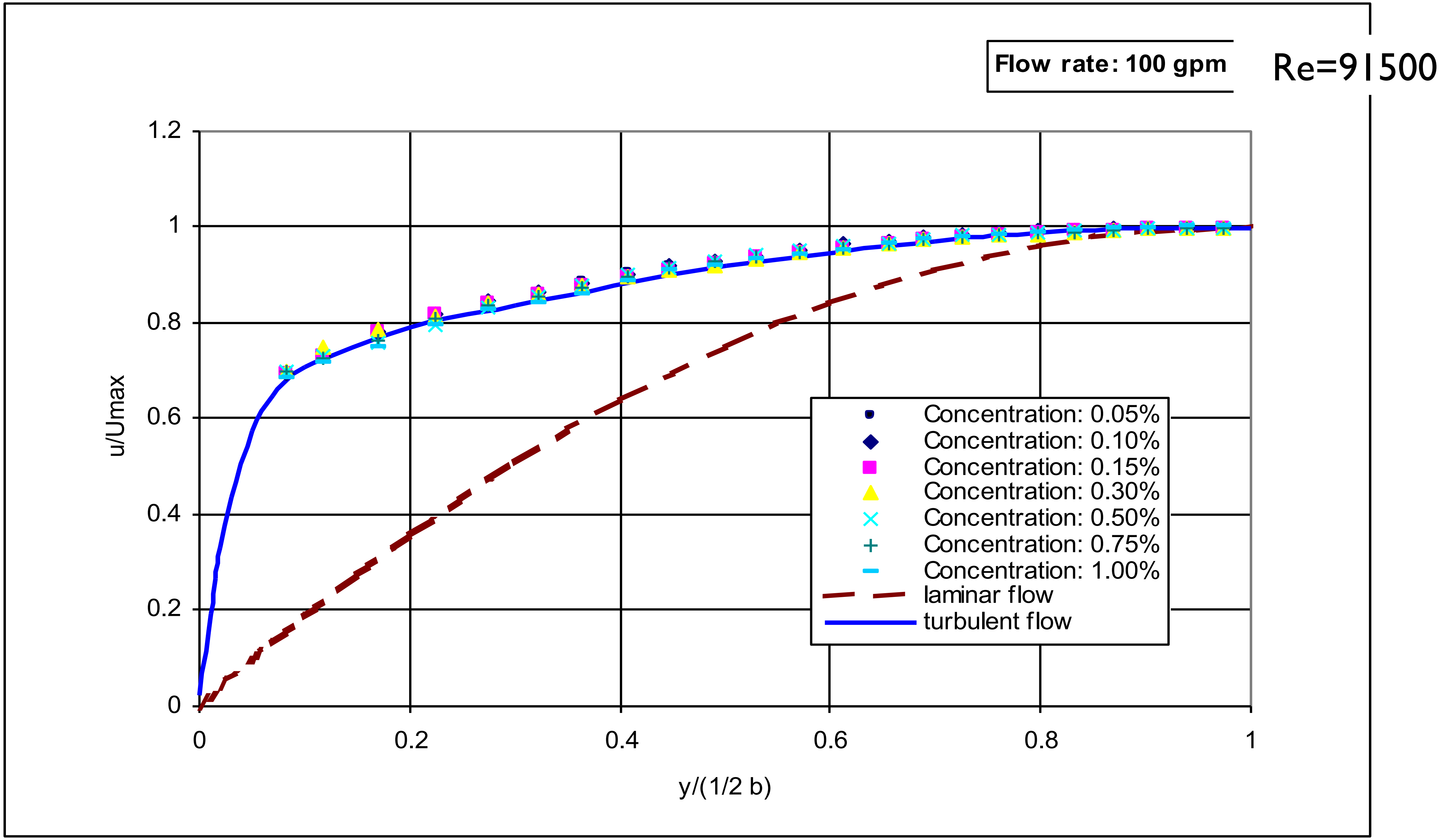

Effect of concentration on velocity profile

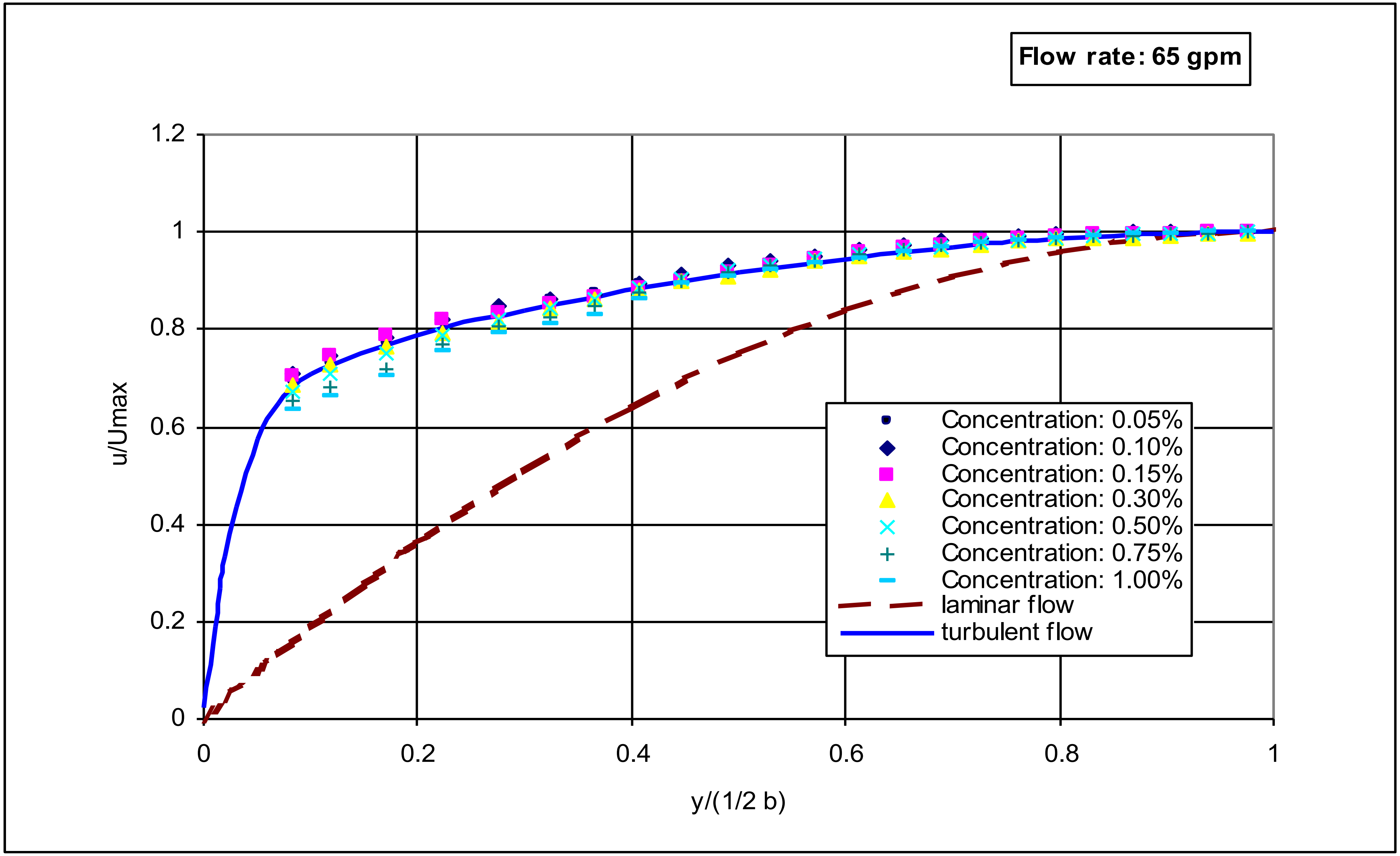

Effect of concentration velocity profile

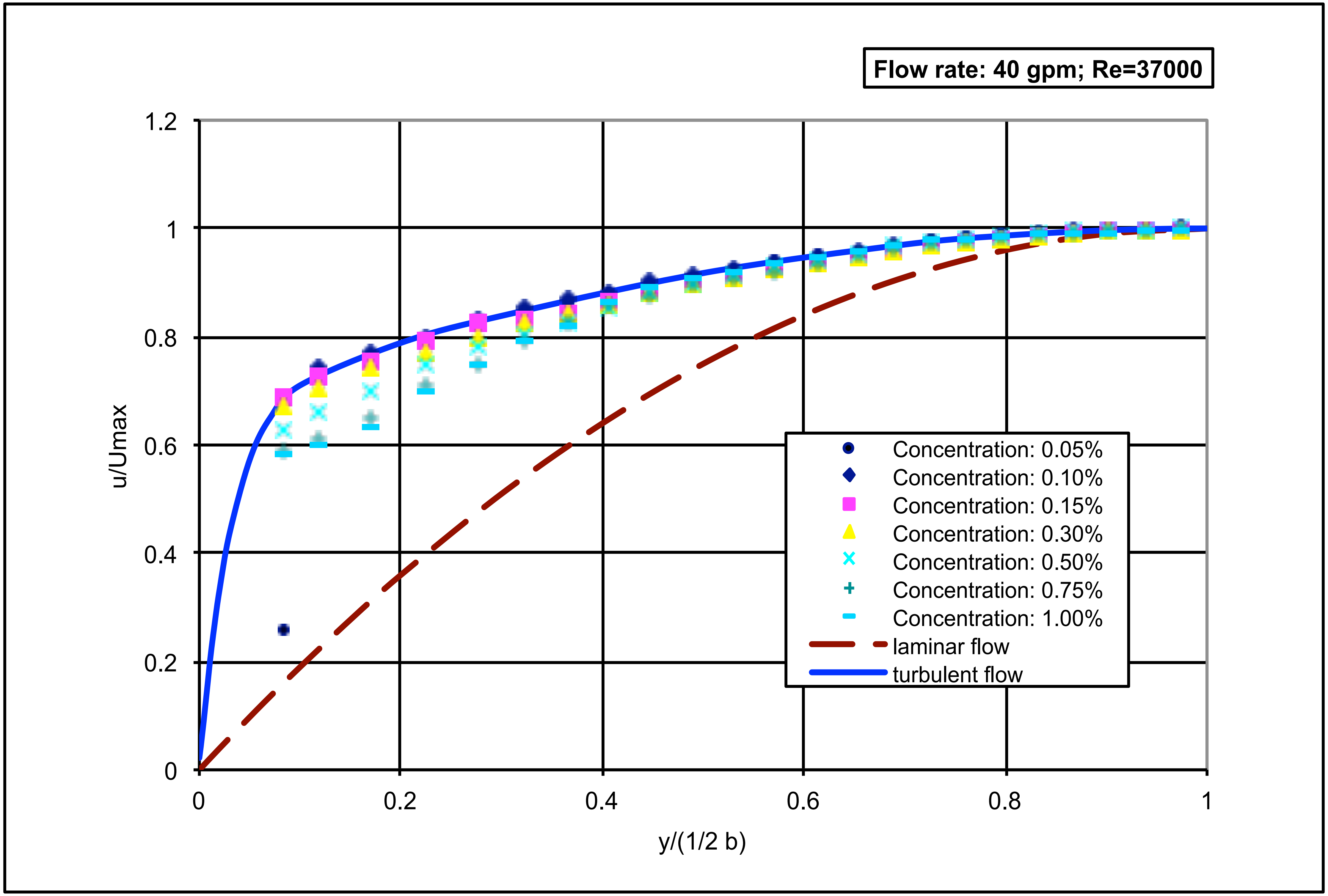

Effect of concentration on velocity profile

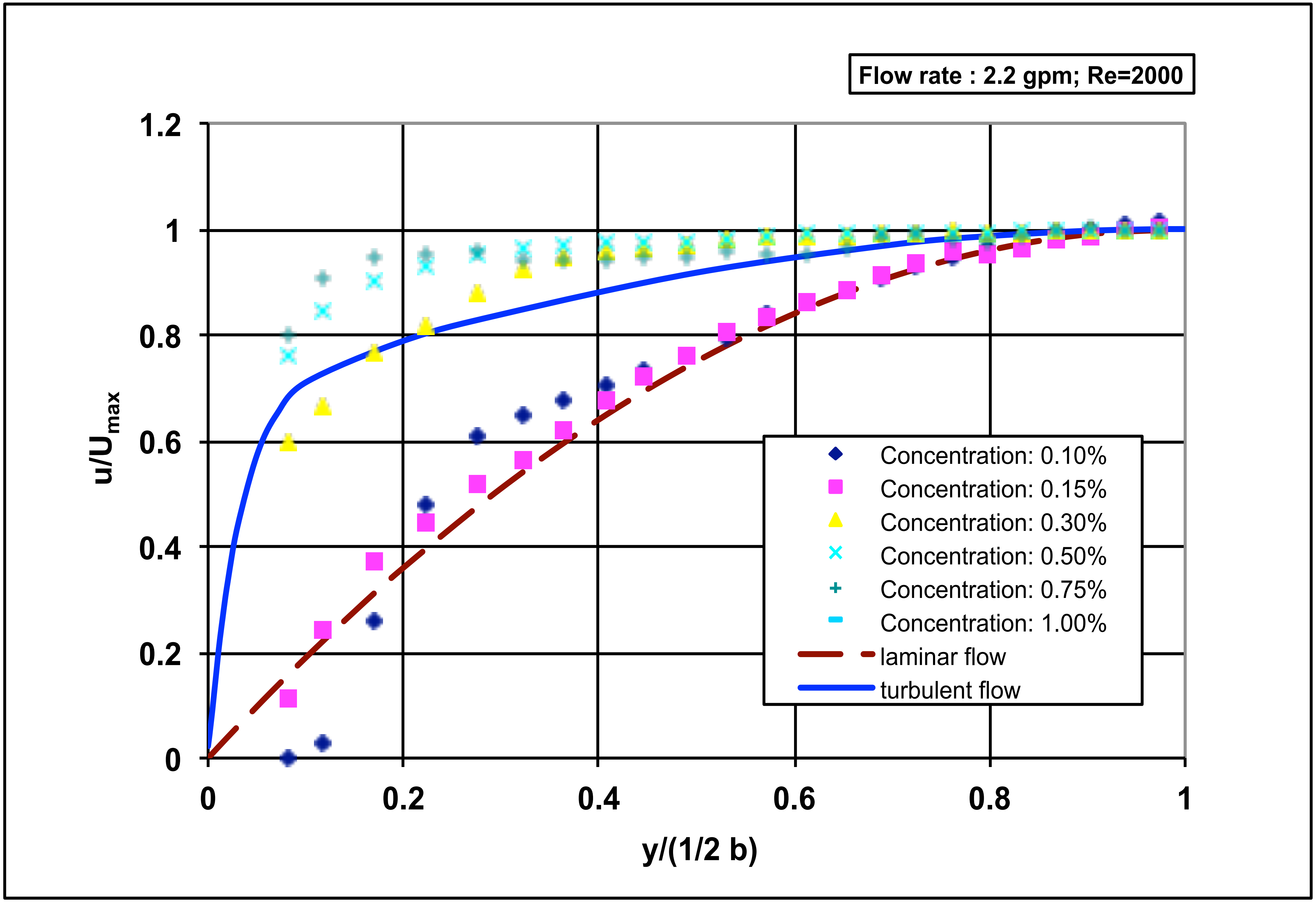

Mean velocity profile for fiber suspension in channel flow

$$u^+ = \frac{1}{0.41}\ln(y^+) + 4.69 + \frac{\Pi}{0.41}\sin^2\left(\frac{y}{0.9b}\pi\right)$$

$$\Pi = 0.98\exp(0.14(nl^3) - 1.9 * 10^{-5} * \mathrm{Re})$$

reduced velocity profile at nl^3 =5.0.
Comparison of Experimental data
And predicted velocity profile.

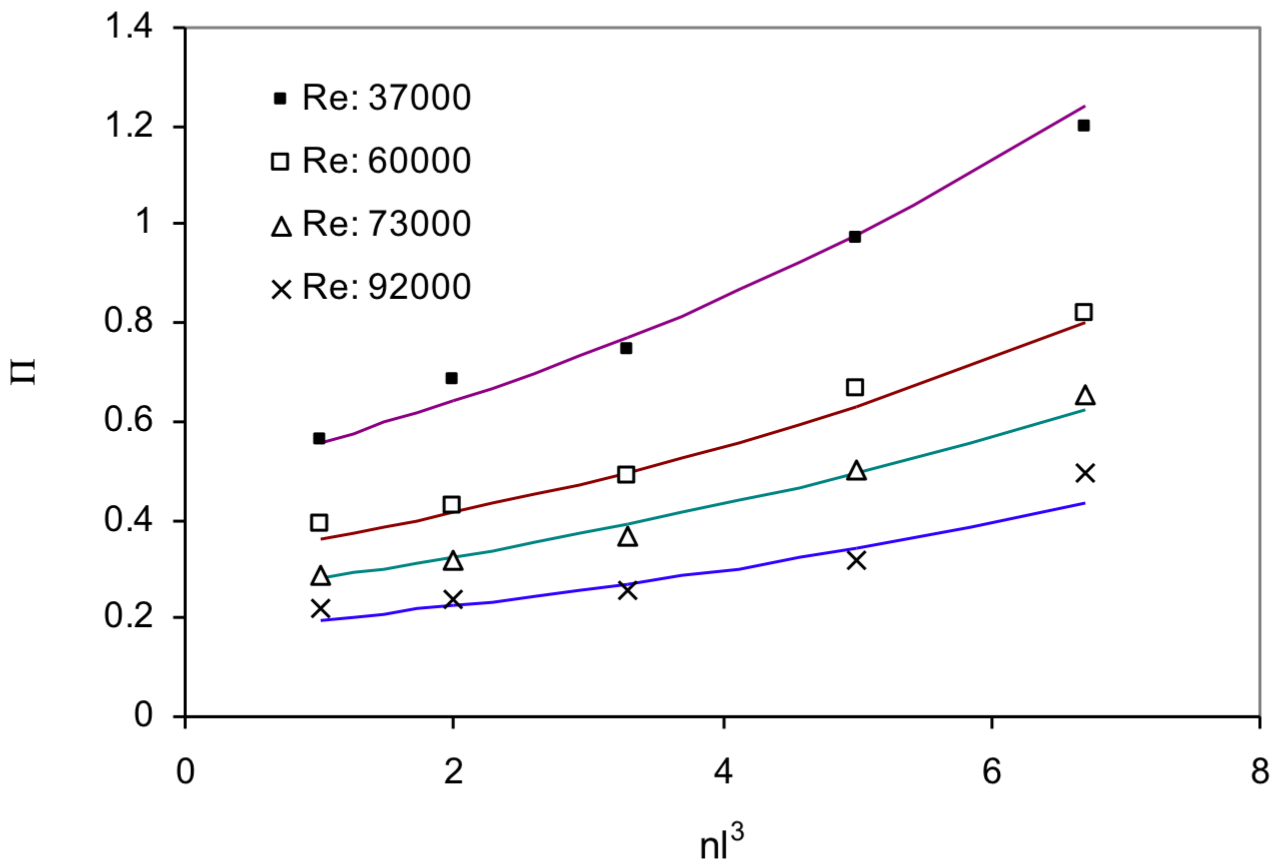

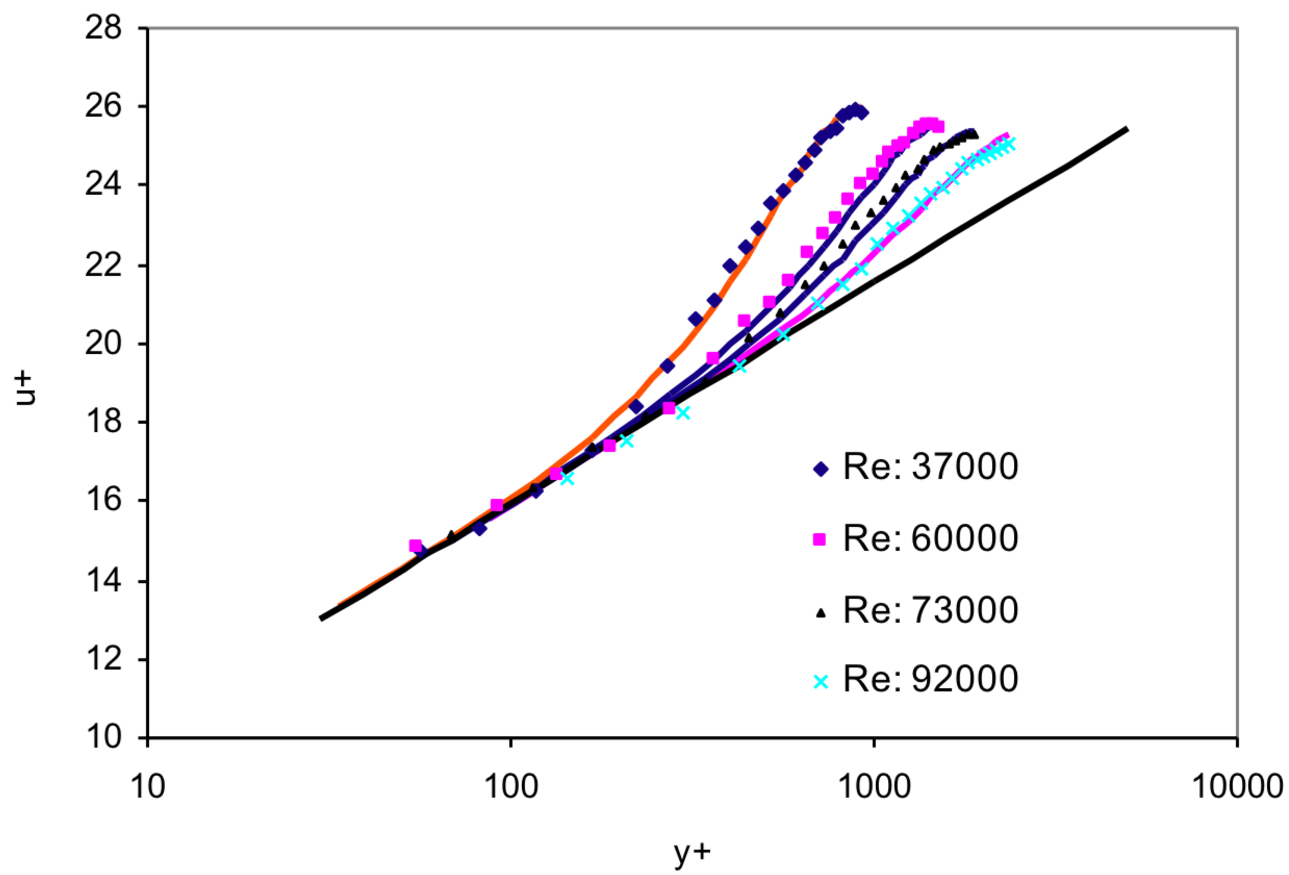

Xu, and Aidun; *Int. J. Multiphase Flow*, 3 1/3, pp. 318-336, 2005

Rigid Fibers

$$\mathrm{Pe} = \frac{\dot{\gamma}\,\mu\,L^3}{k_B T} >> 1 \qquad \mathrm{Re} = \frac{\rho\dot{\gamma}\,L^2}{\mu} << 1$$

$$\eta = \frac{\mu_{eff}}{\mu} = 1 + F(c_{vf}, r_p;\ p(\phi))$$

r_p aspect ratio;

$p(\phi)$ orienation dist.

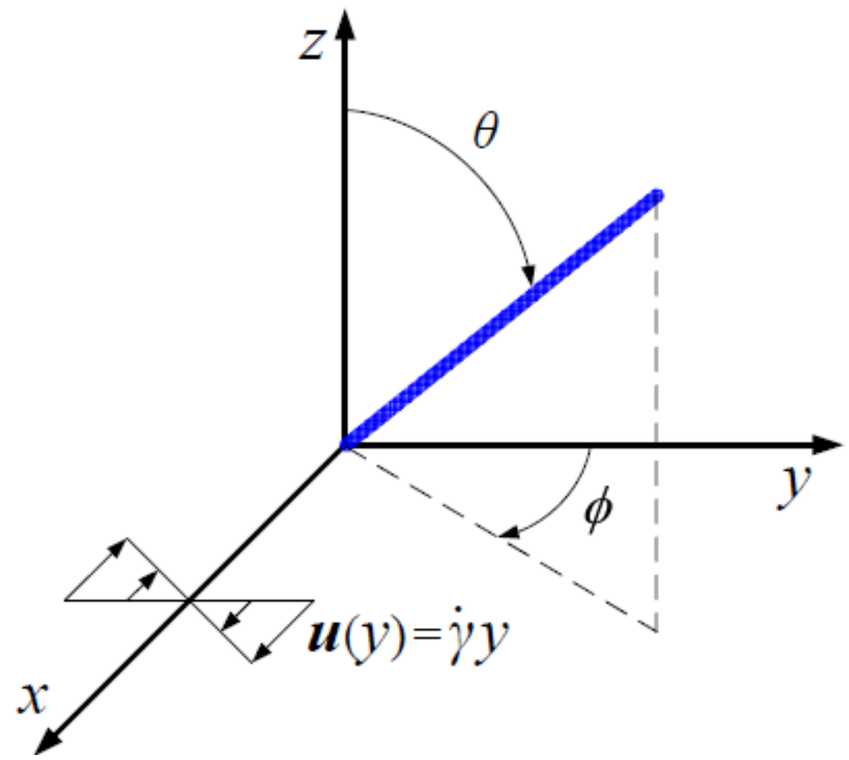

$$\Sigma = -P\mathbf{I} + 2\mu\mathbf{E} + \mu_f\left(\langle\mathbf{pppp}\rangle - \frac{1}{3}\mathbf{I}\langle\mathbf{pp}\rangle\right):\mathbf{E}$$

$$\mu_{eff} = \frac{\Sigma_{12}}{2\mu E_{12}}$$

μ_f depends on $c_{vf}, p(\phi), r_p$

$$\mathbf{p} = \mathrm{p_x}\mathbf{e}_x + \mathrm{p_y}\mathbf{e}_y + \mathrm{p_z}\mathbf{e}_z$$

$$N_1 = \Sigma_{xx} - \Sigma_{yy}$$

$$N_2 = \Sigma_{yy} - \Sigma_{zz}$$

For deformable fibers, concept of *Bending Ratio* (*BR*)

Critical shear-induced buckling stress,

$$(\mu\dot{\gamma})_{crit} = \frac{E_Y\left(\ln(2r_e) - 1.5\right)}{2r_p^4}$$

(Forgacs and Mason, *J. Col. Sci.*, 1959)

E_Y , Young's Modulus

L , fiber length

D , fiber diameter

$r_p = L/D$

r_e , effective aspect ratio

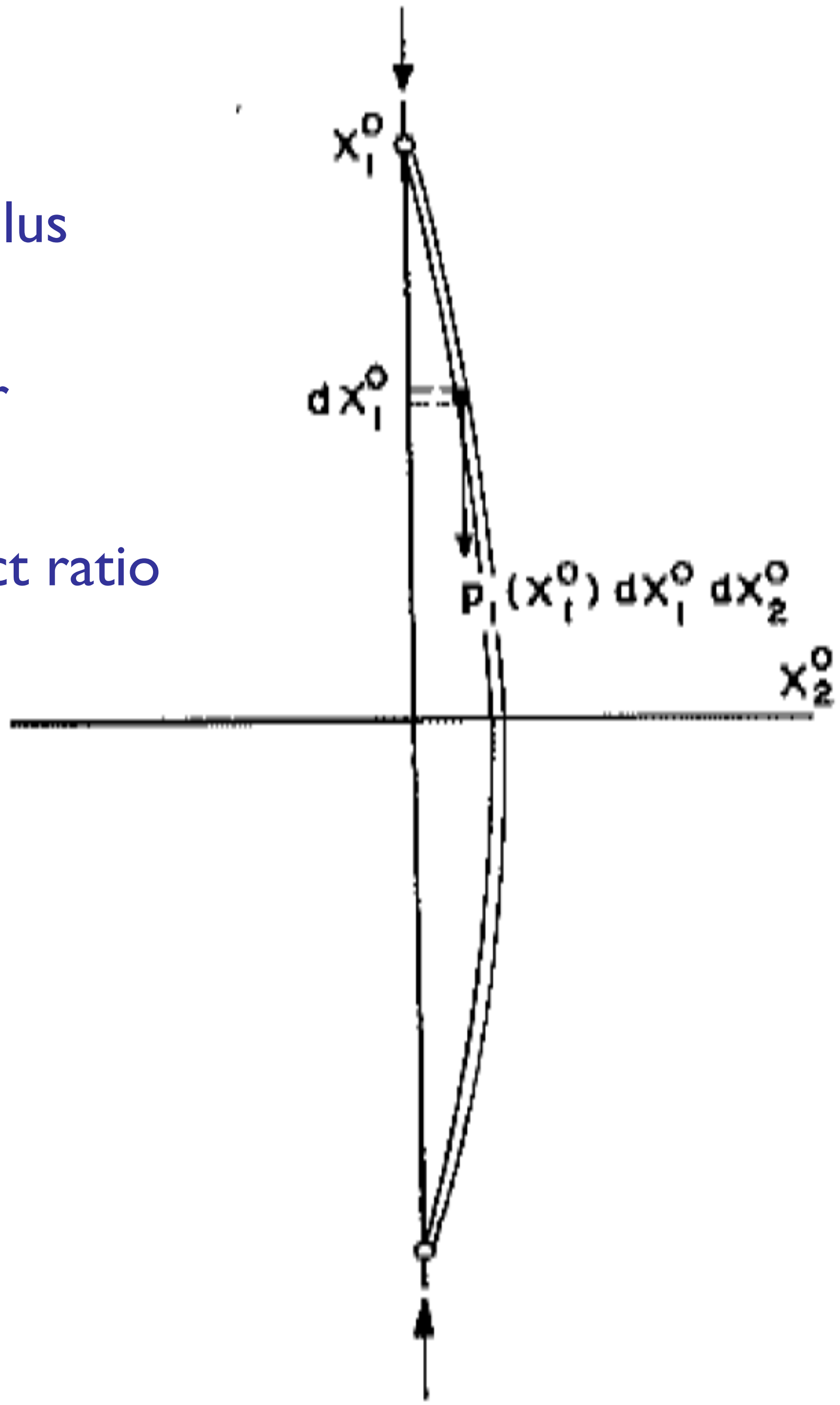

For deformable fibers, concept of *Bending Ratio* (*BR*)

Critical shear-induced buckling stress,

$$(\mu\dot{\gamma})_{crit} = \frac{E_Y\left(\ln(2r_e) - 1.5\right)}{2r_p^4}$$

(Forgacs and Mason, *J. Col. Sci.*, 1959)

E_Y , Young's Modulus

L , fiber length

D , fiber diameter

$r_p = L/D$

r_e , effective aspect ratio

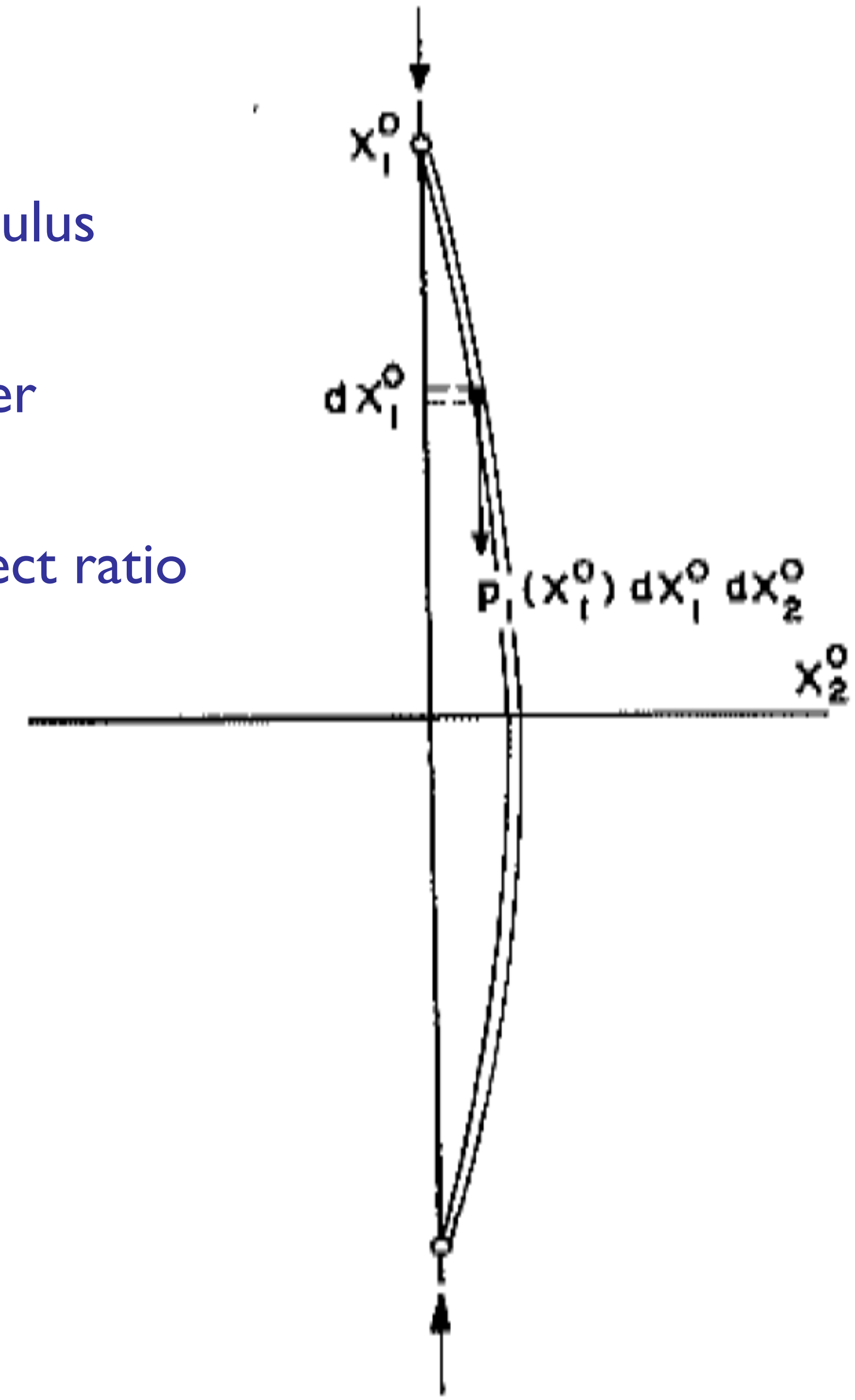

$$BR = \frac{E_Y\left(\ln(2r_e) - 1.5\right)}{2(\mu\dot{\gamma})r_p^4}$$

$$\eta = \frac{\mu_{eff}}{\mu} = 1 + F(c_{vf}, r_p, BR; p(\phi))$$

Lattice-Boltzmann Method

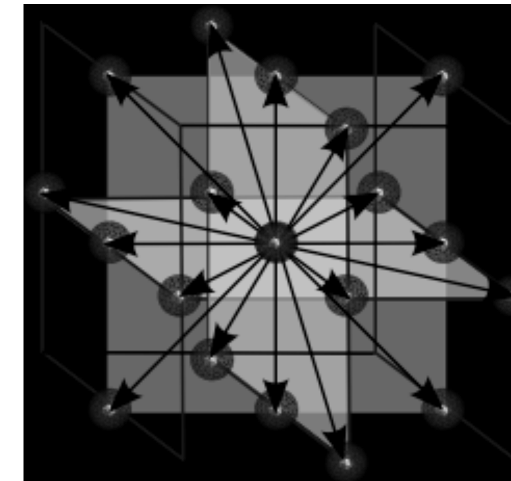

D3Q19
LB Stencil

Discrete Boltzmann equation:

$$f_i(\mathbf{r}+\mathbf{e}_i, t+1) = f_i(\mathbf{r}, t) - \frac{1}{\tau}\Big(f_i(\mathbf{r}, t) - f_i^{(eq)}(\mathbf{r}, t)\Big)$$

Macroscopic properties related to moments of distribution:

Density

$$\sum_{i=1}^{Q} f_i^{(eq)}(\mathbf{r}, t) = \rho$$

Momentum

$$\sum_{i=1}^{Q} f_i^{(eq)}(\mathbf{r}, t)\mathbf{e}_i = \rho\mathbf{u}$$

Pressure

$$\sum_{i=1}^{Q} f_i^{(eq)}(\mathbf{r}, t)\mathbf{e}_i\mathbf{e}_i = c_s^2\rho\mathbf{I} + \rho\mathbf{u}\mathbf{u}$$

Symbols

$\mathbf{r} =$	position vector
$\mathbf{e}_i =$	lattice direction vector
$f_i =$	fluid distribution
$f_i^{(eq)} =$	equilibrium fluid distribution
$\rho =$	density
$\mathbf{x} =$	nodal displacement
$\mathbf{I} =$	identity tensor
$\mathbf{u} =$	fluid velocity
$\tau =$	relaxation time

Aidun & Clausen. ***Annual Rev. Fluid Mech., 42, 2010.***

Flexible fiber model

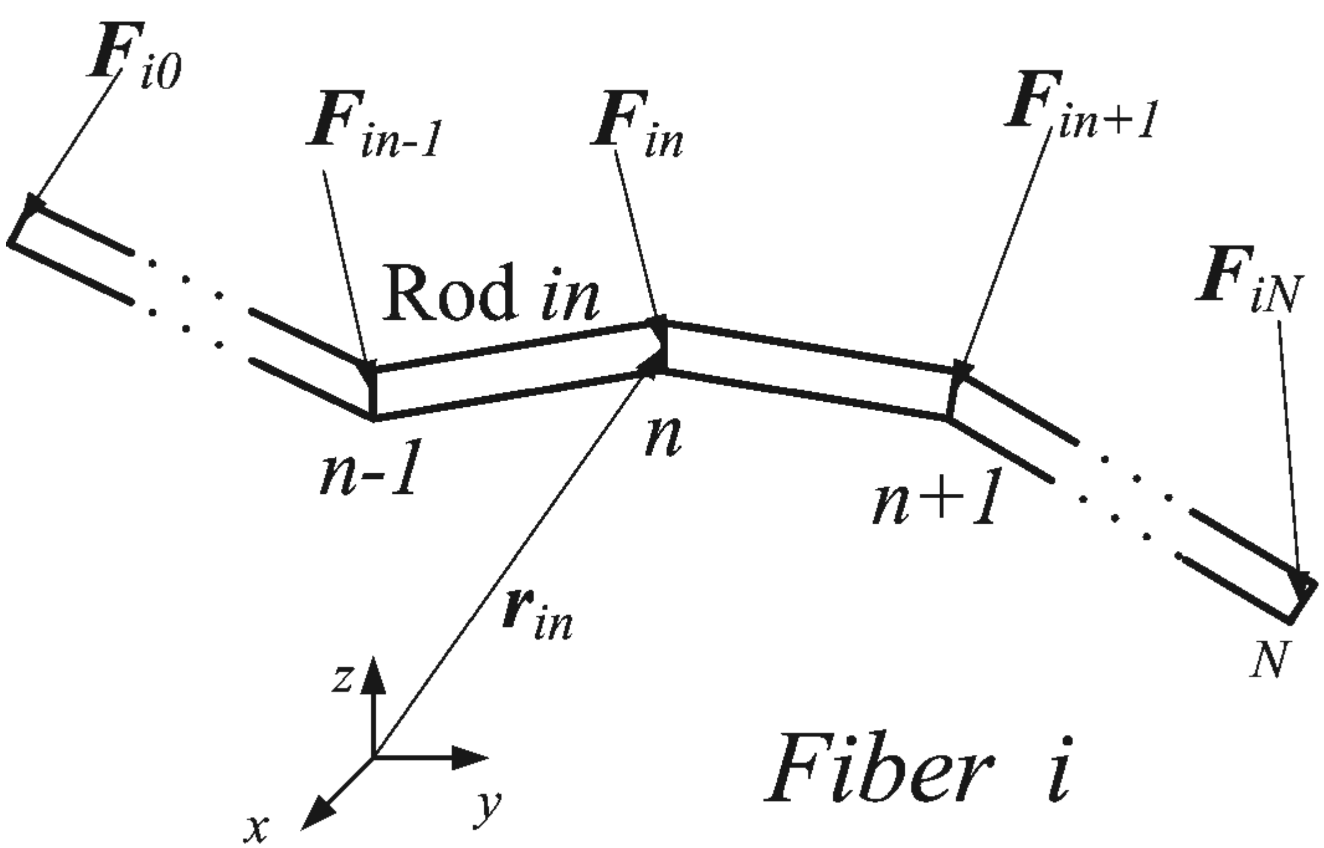

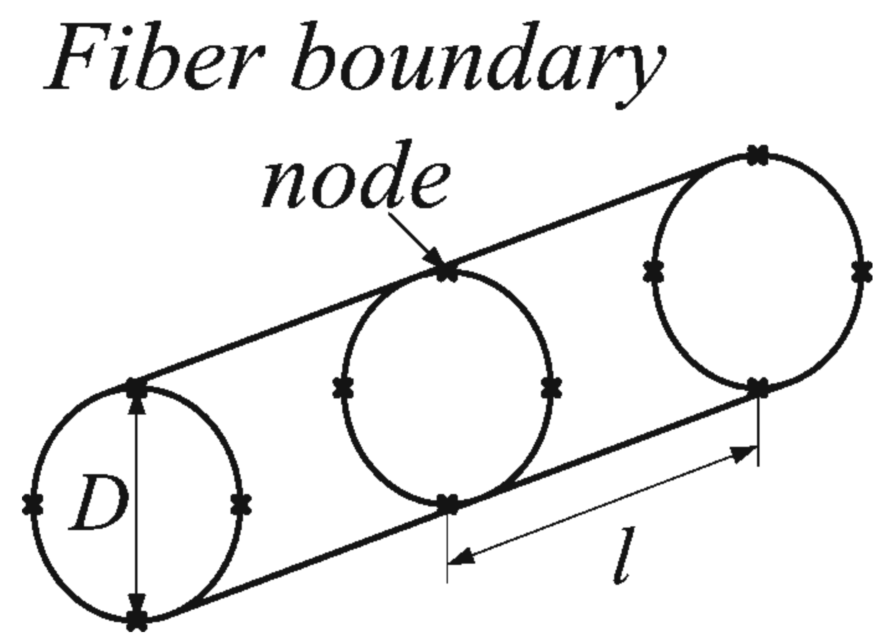

$$F_i = \sum F_{in}$$

$$F_{in}^{mov} = F_i / (N+1) \qquad \text{and} \; F_{in}^{def} = F_{in} - F_{in}^{mov}$$

$$dl_{in} = \frac{1}{E_Y(\pi D^2/4)} \left[p_{in} \cdot \left(F_{in}^{def} - F_{in-1}^{def} \right) \right]$$

: position vector of *n*th hinge of fiber *i*

: unit vector parallel to axis of rod *in*

$$p_{in} = \frac{r_{in} - r_{in-1}}{\left| r_{in} - r_{in-1} \right|}$$

Wu and Aidun, *Int. J. Multiphase Flow*, 2009

External Boundary Force (EBF)

The no-slip boundary condition on the surface of the particle is satisfied by the requirement that the fluid velocity at the solid boundary node is equal to the solid velocity at that point.

$$\boldsymbol{U}_f\left(\boldsymbol{x}^l,\ t\right) = \int \boldsymbol{u}\left(\boldsymbol{x}^e,\ t\right) D\left(\boldsymbol{x}^e - \boldsymbol{x}^l\right) d\,\boldsymbol{x}^e$$

$\boldsymbol{x}^e$: Eulerian position vector for fluid nodes

$\boldsymbol{x}^l$: Lagrangian position vector for solid nodes

$\boldsymbol{u}(\boldsymbol{x}^e, t)$: discrete fluid velocity

$\boldsymbol{U}_f$: fluid velocity at solid boundary nodes

$\boldsymbol{U}_p$: solid velocity at solid boundary nodes

D : Dirac delta function

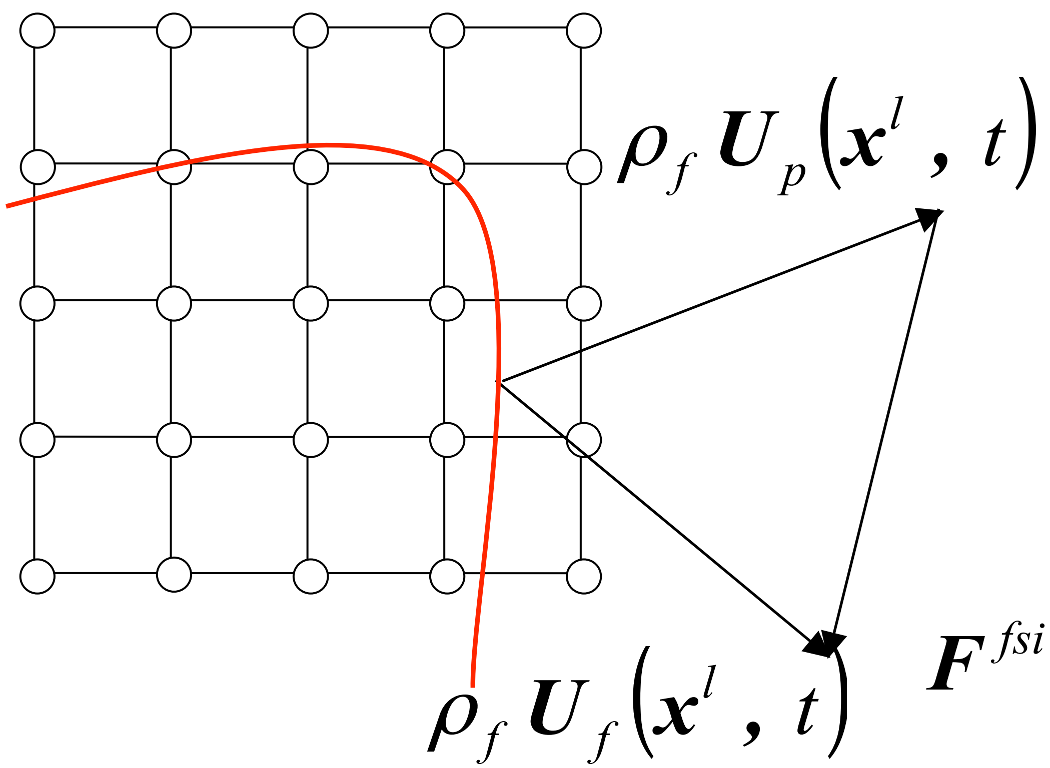

$$\boldsymbol{F}^{fsi}\left(\boldsymbol{x}^l,\ t\right) = \left(\rho_f\,\boldsymbol{U}_f\left(\boldsymbol{x}^l,\ t\right) - \rho_f\,\boldsymbol{U}_p\left(\boldsymbol{x}^l,\ t\right)\right)/\Delta t$$

Wu and Aidun, *Int. J. Num. Method Fluids*, 2010

Fiber deformation in shear; BR=40

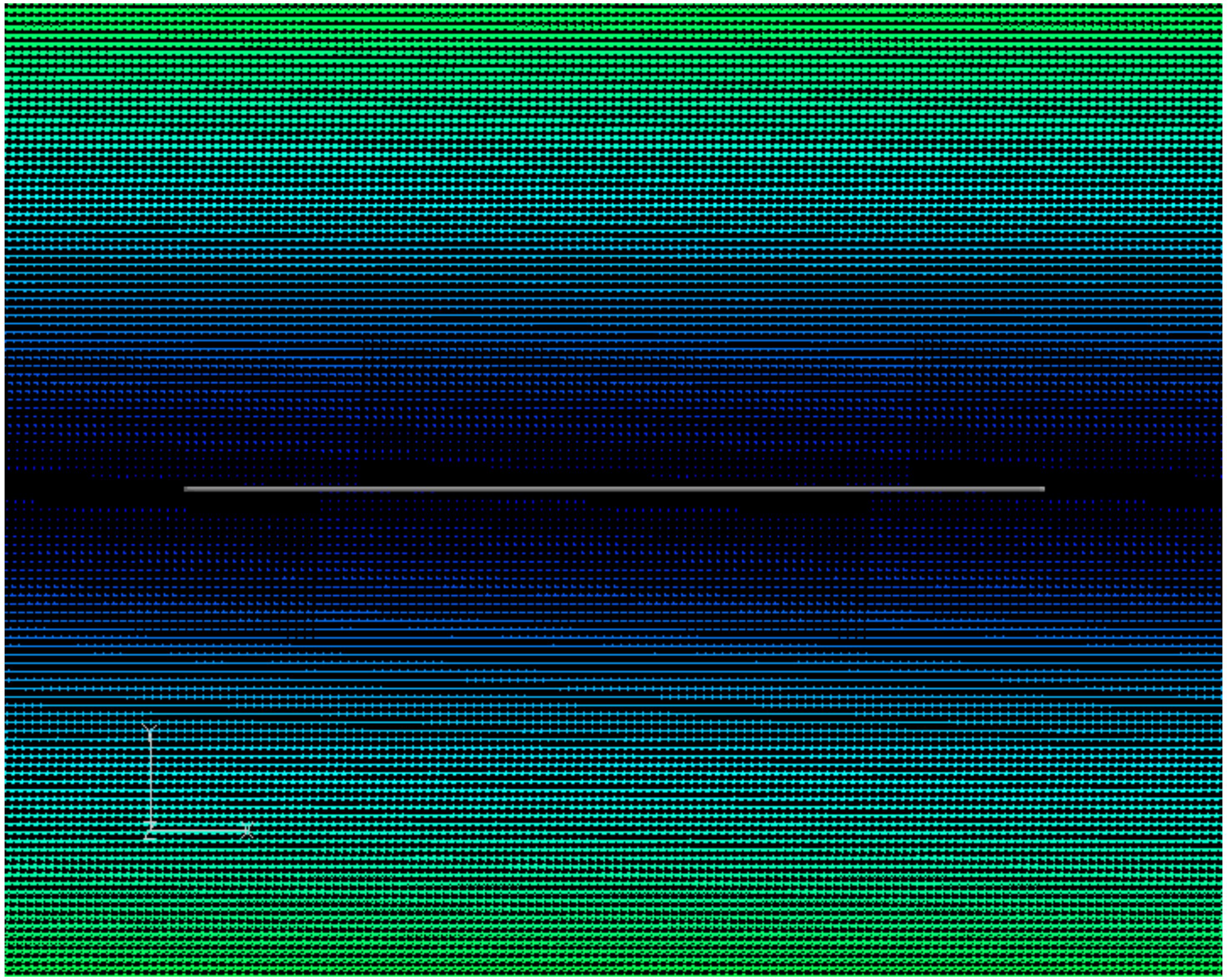

Fiber deformation in shear; BR=0.36

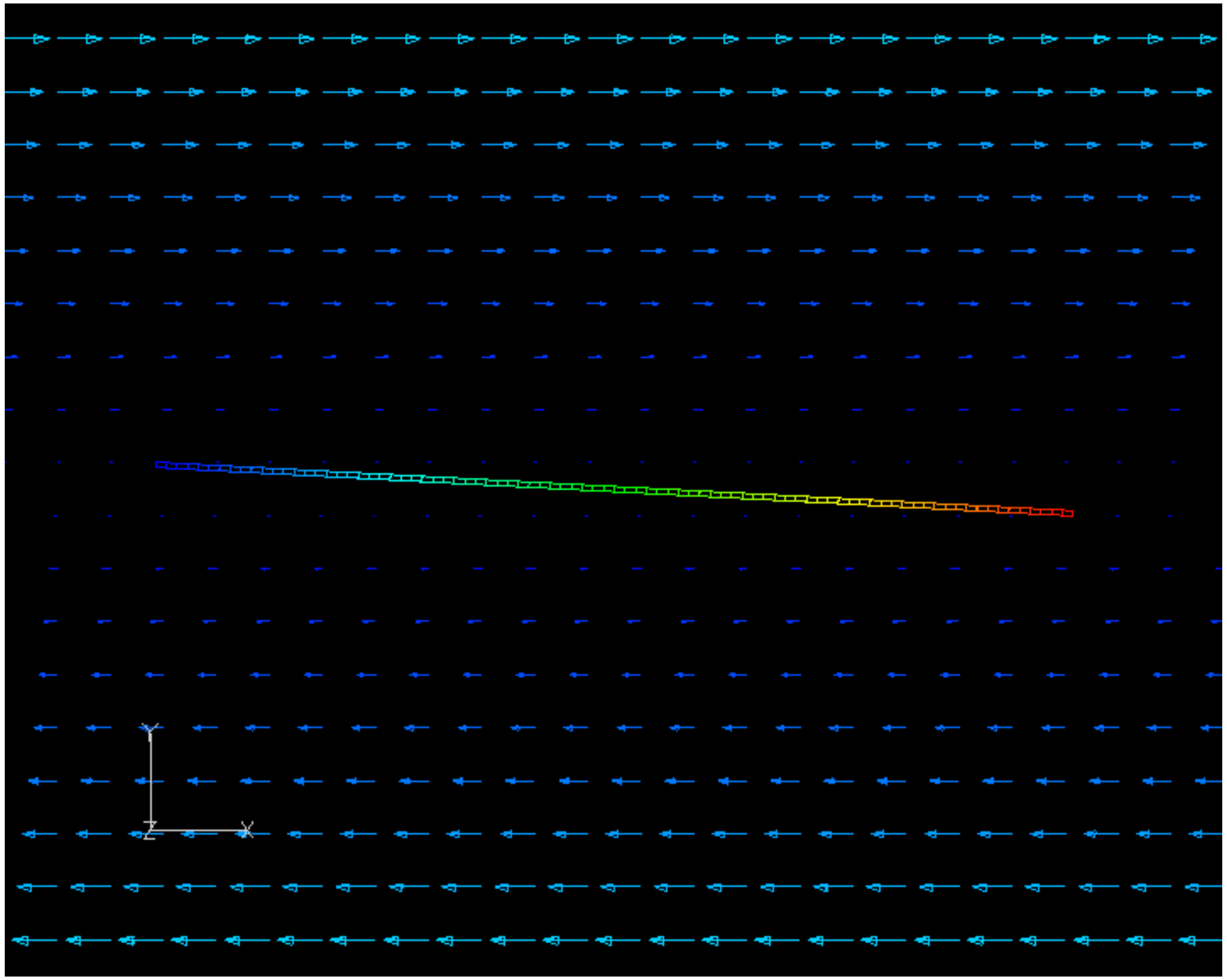

Fiber deformation in shear; BR=0.18

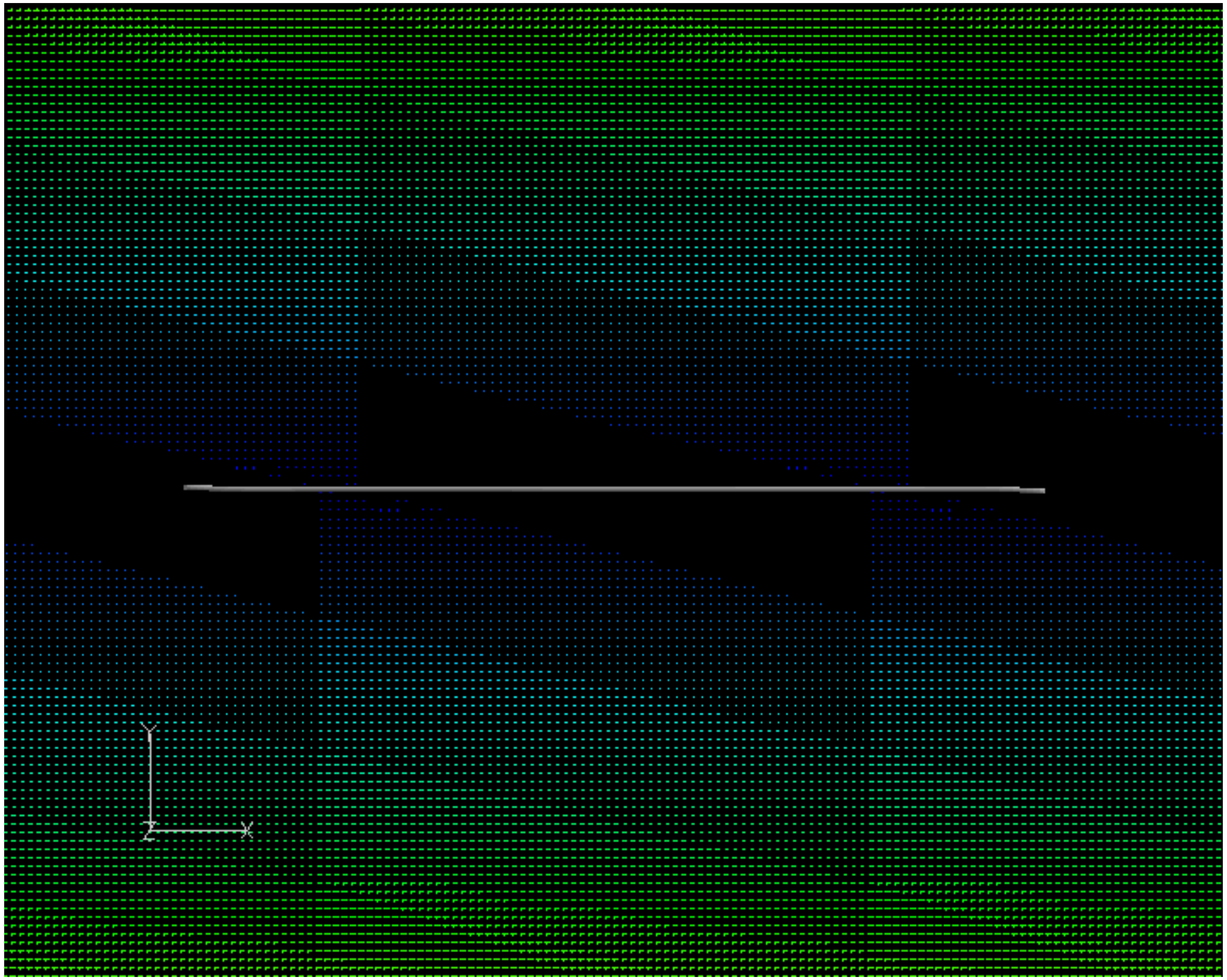

Loci of the end of a Nylon filament (r_p=170) in simple shear flow

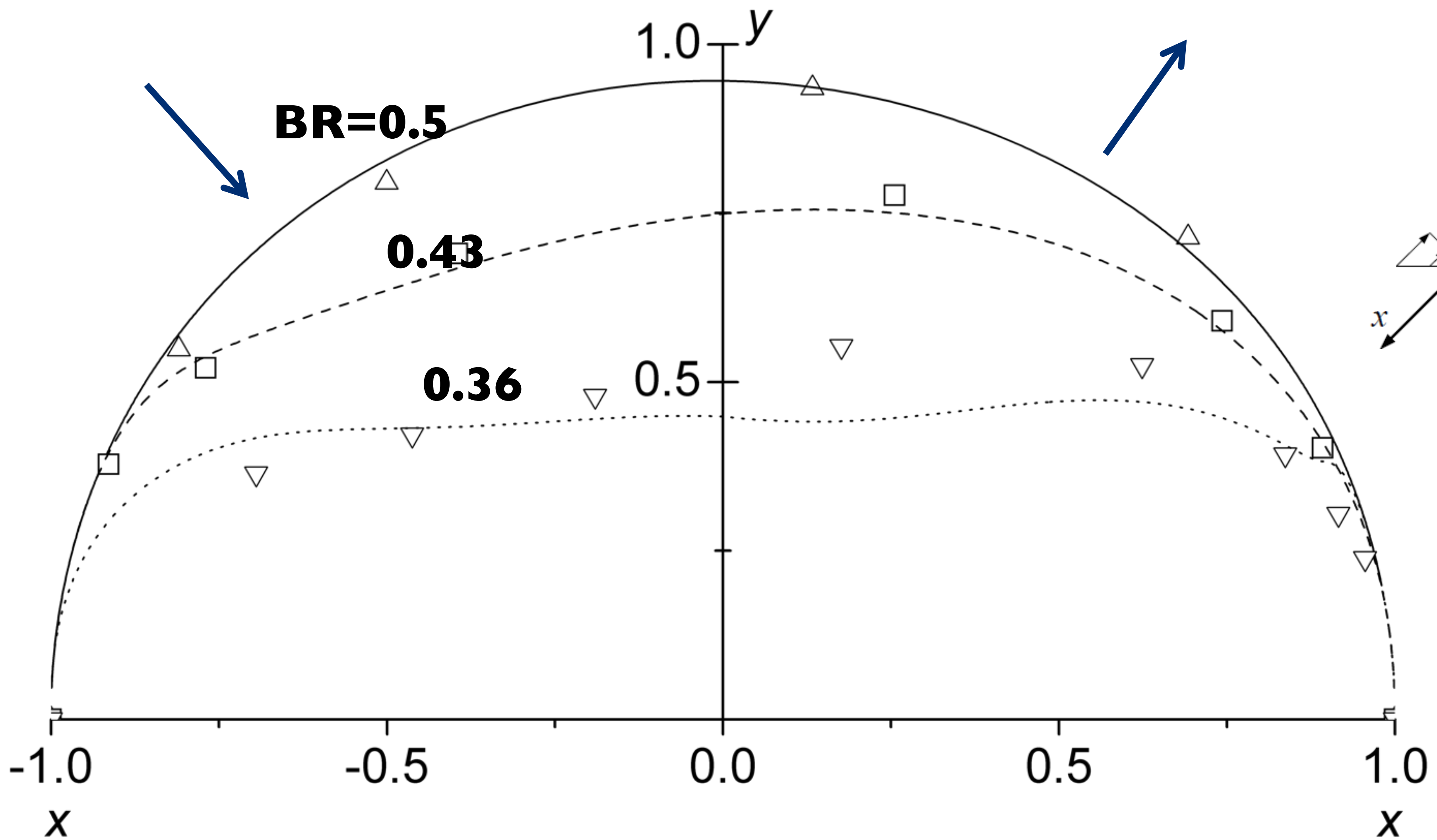

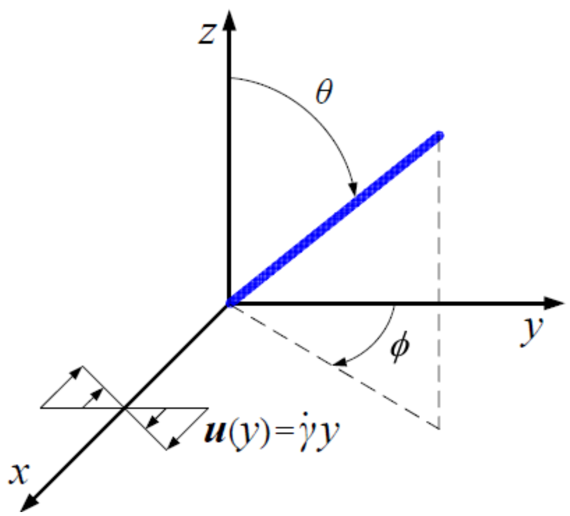

Symbols are the experimentall data of Forgacs and Mason (1959) for BR=0.5, 0.43 and 0.35. Lines are the corresponding LB-EBF simulation results (Wu and Adiun, 2010).

LB-EBF Simulation of deformable fibers

Fiber diameter $D = 0.12\text{mm}$, r_p=16 $\mu = 13\text{Pa s}$

$BR >> 1$

$BR = 0.3$

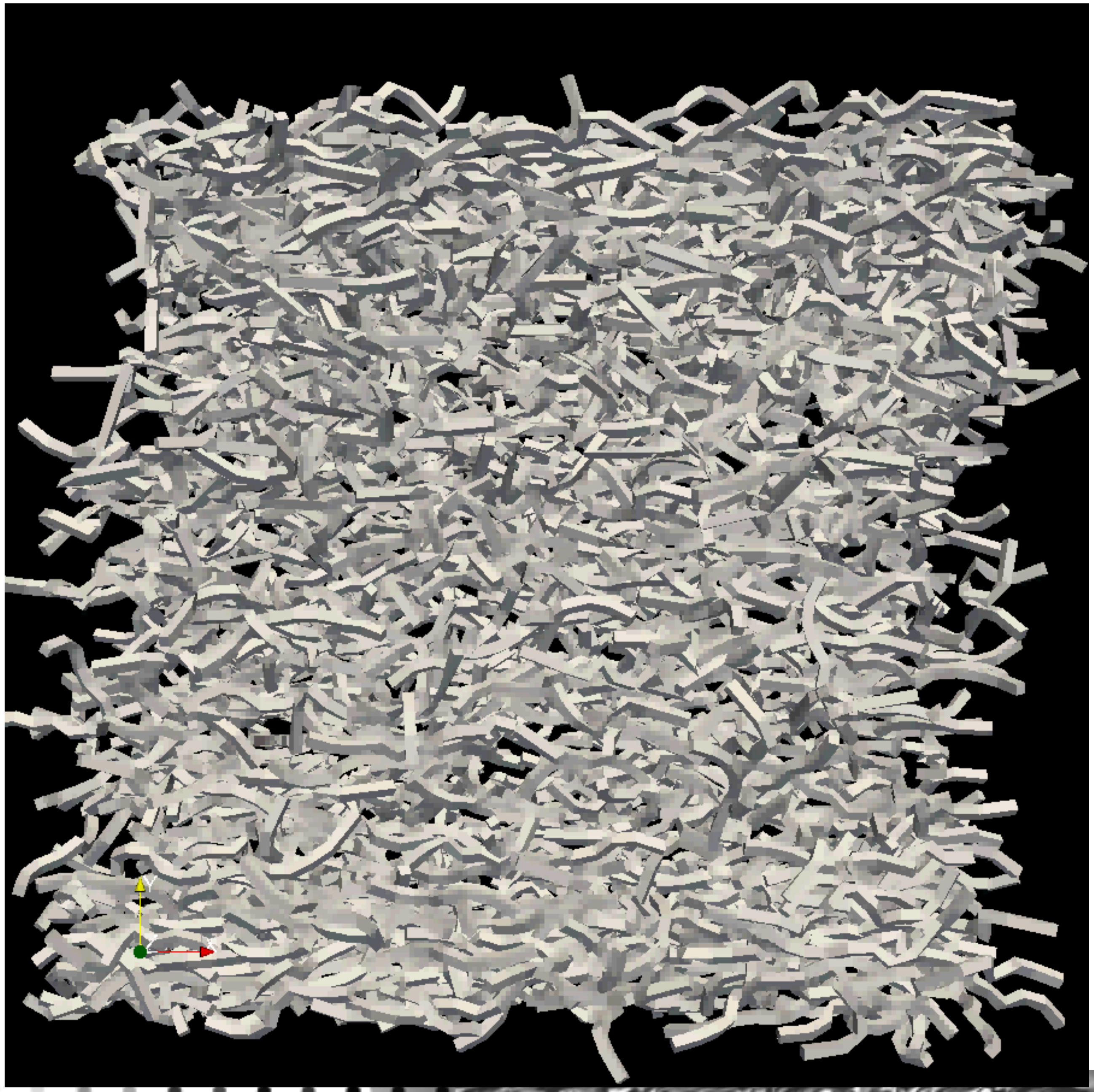

Relative viscosity

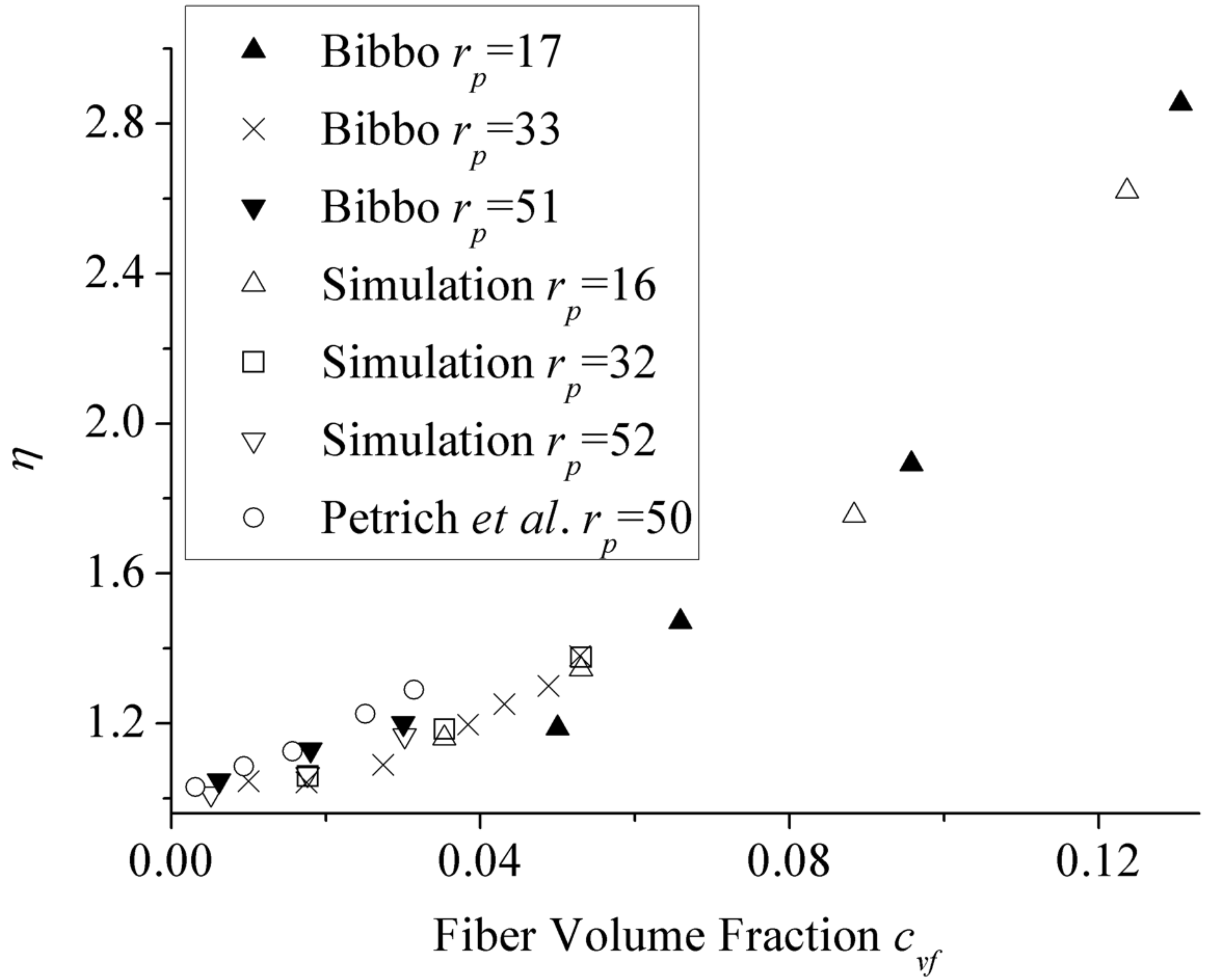

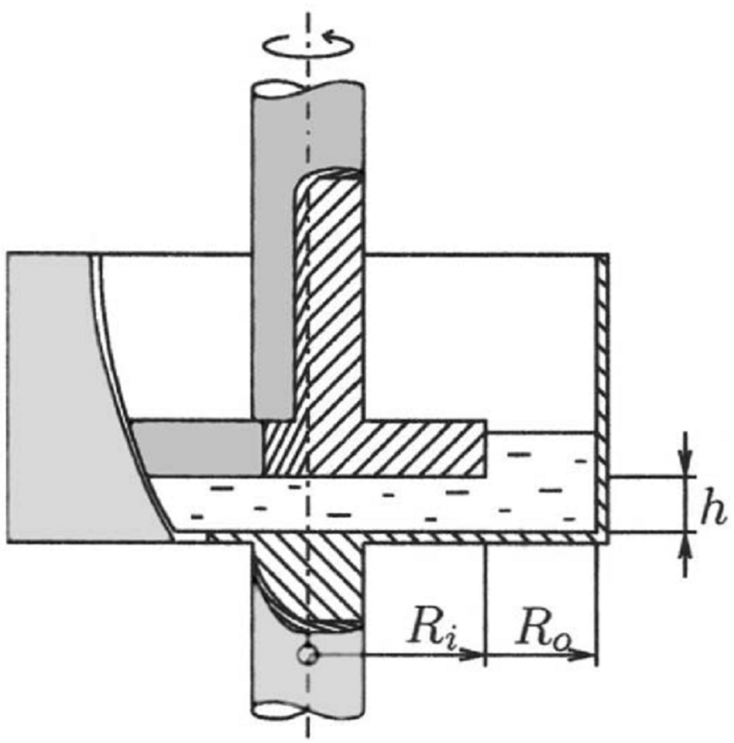

Fiber diameter $D = 0.12\text{mm}$ $c_{vf} = 0.0051 \sim 0.124$ $E_Y = 3\text{GPa}$ $\mu = 13\text{Pa s}$

Bibbo *PhD thesis*, MIT 1987
Petrich et al., J. Non-Newtonian F. M., 2000

Relative viscosity & orientation distribution

Fiber diameter $D = 0.12\text{mm}$ r_p=16 $\mu = 13\text{Pa s}$

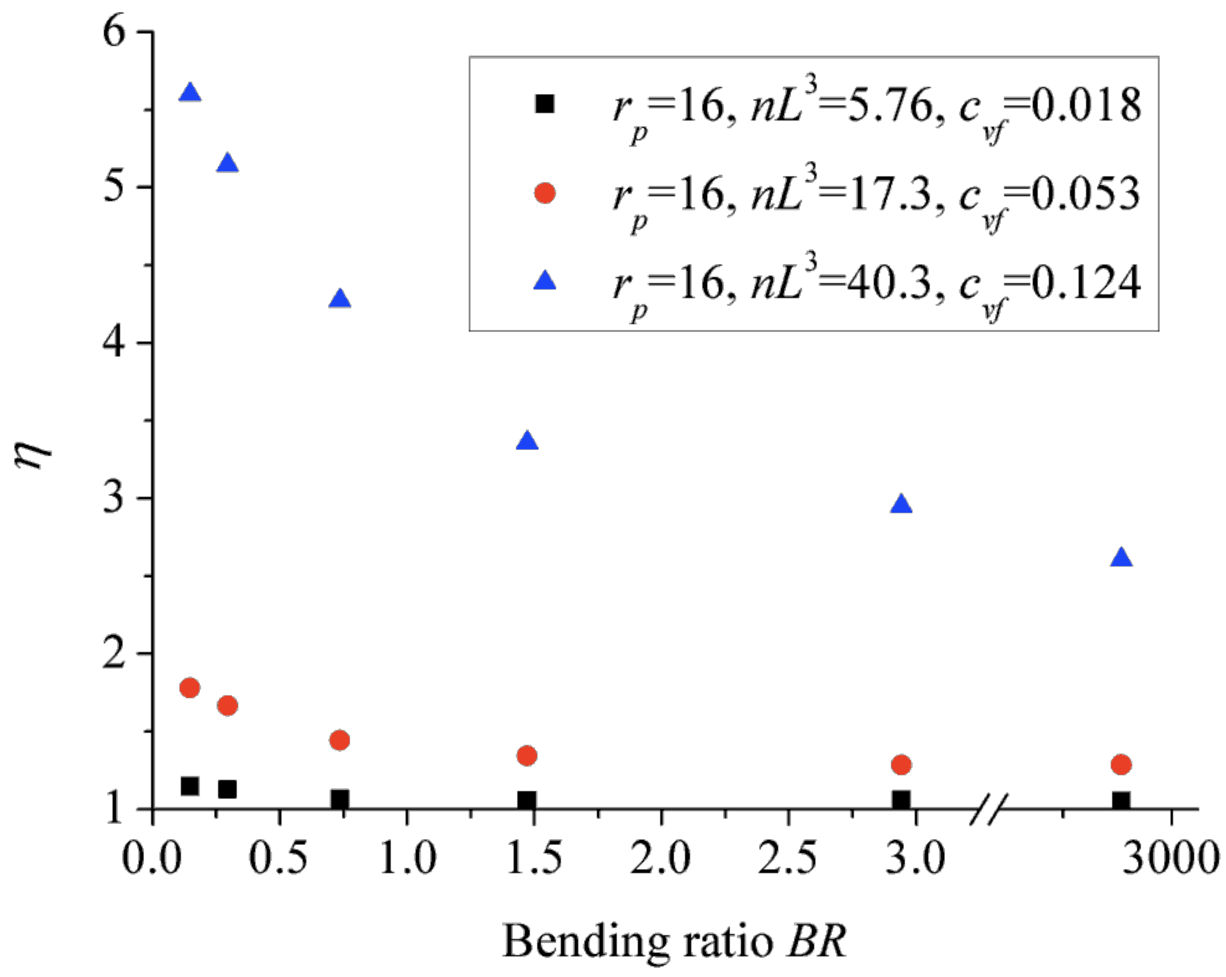

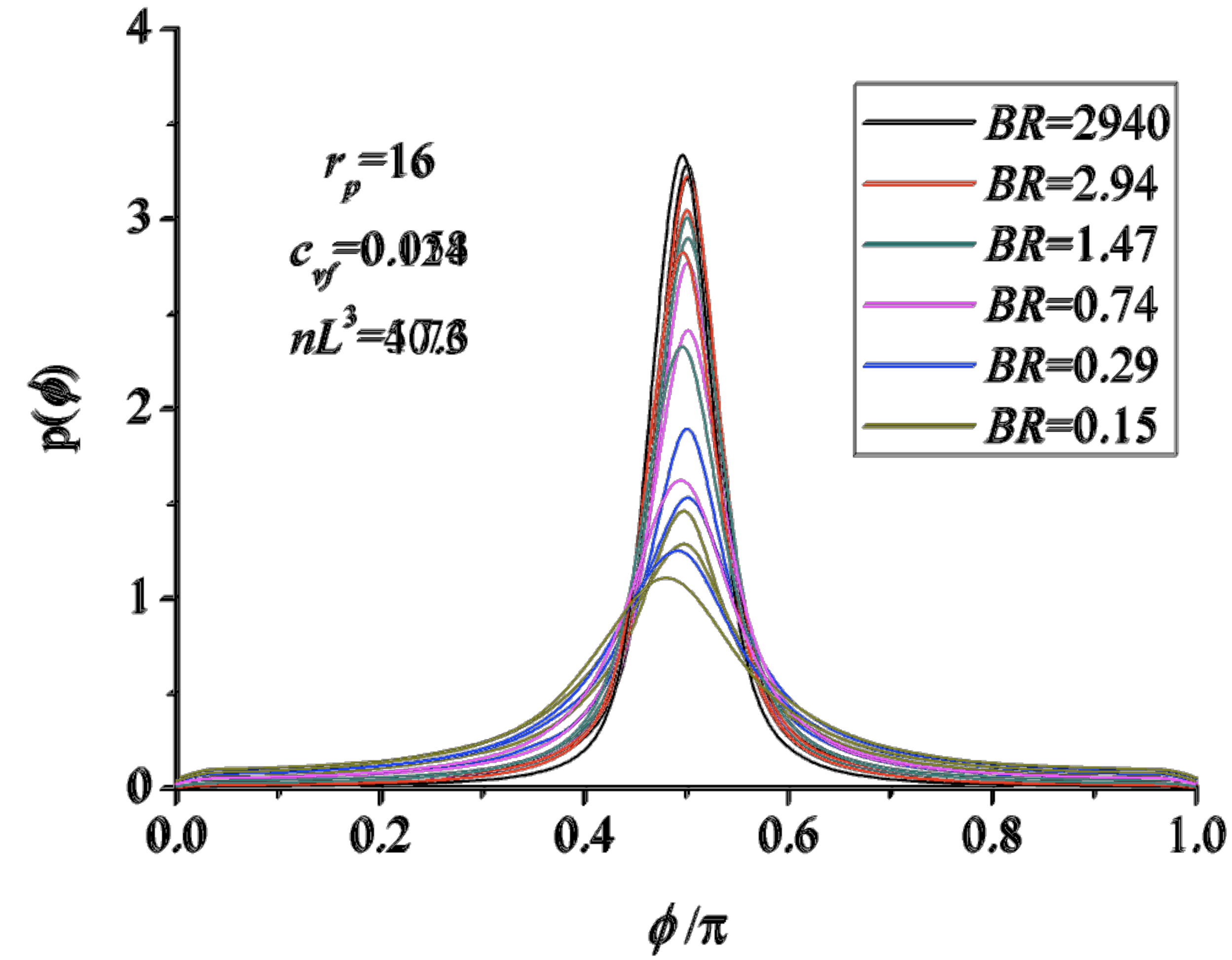

Primary Normal stress difference, N_1

fiber diameter $D = 0.12\text{mm}$ r_p=16 $\mu = 13\text{Pa s}$

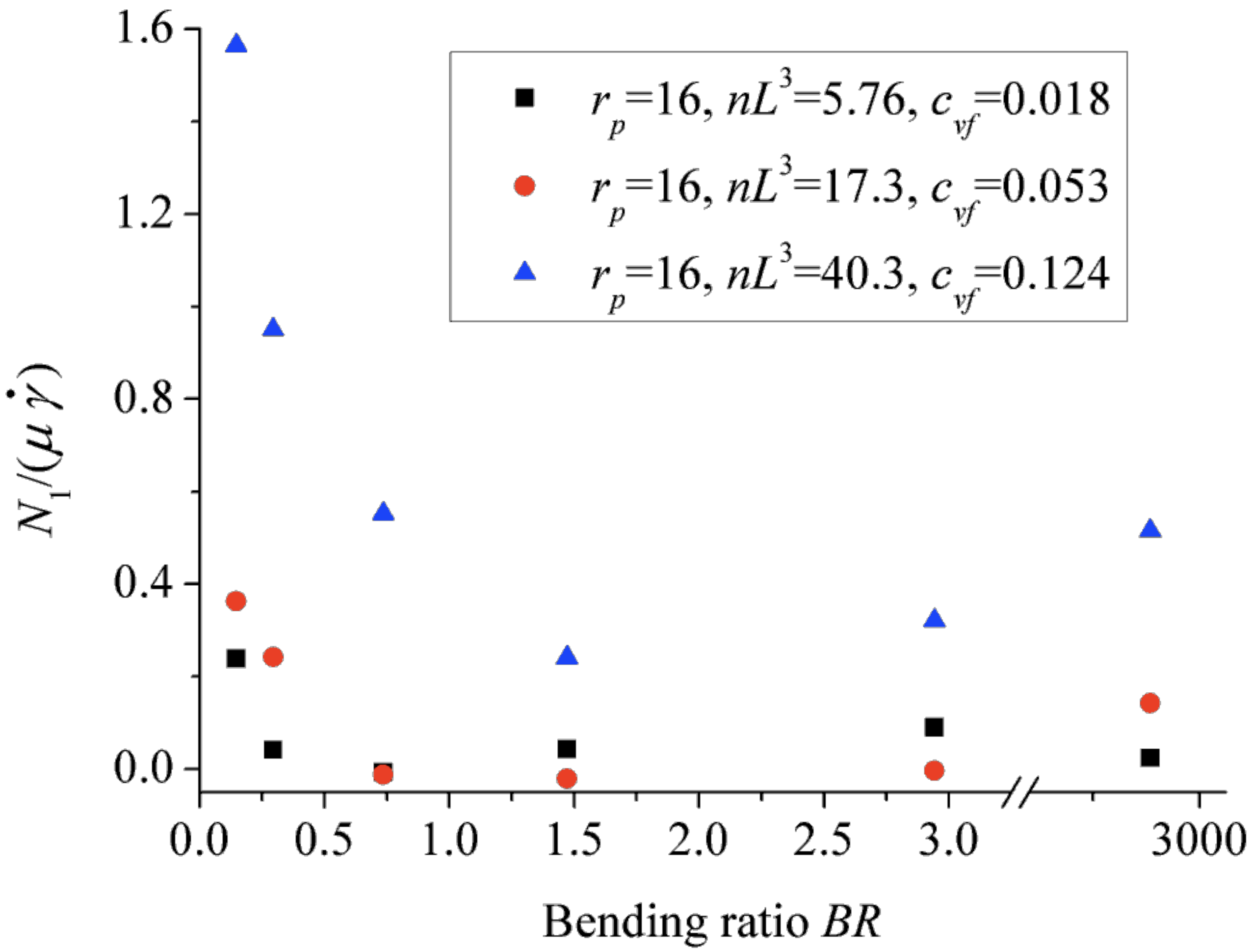

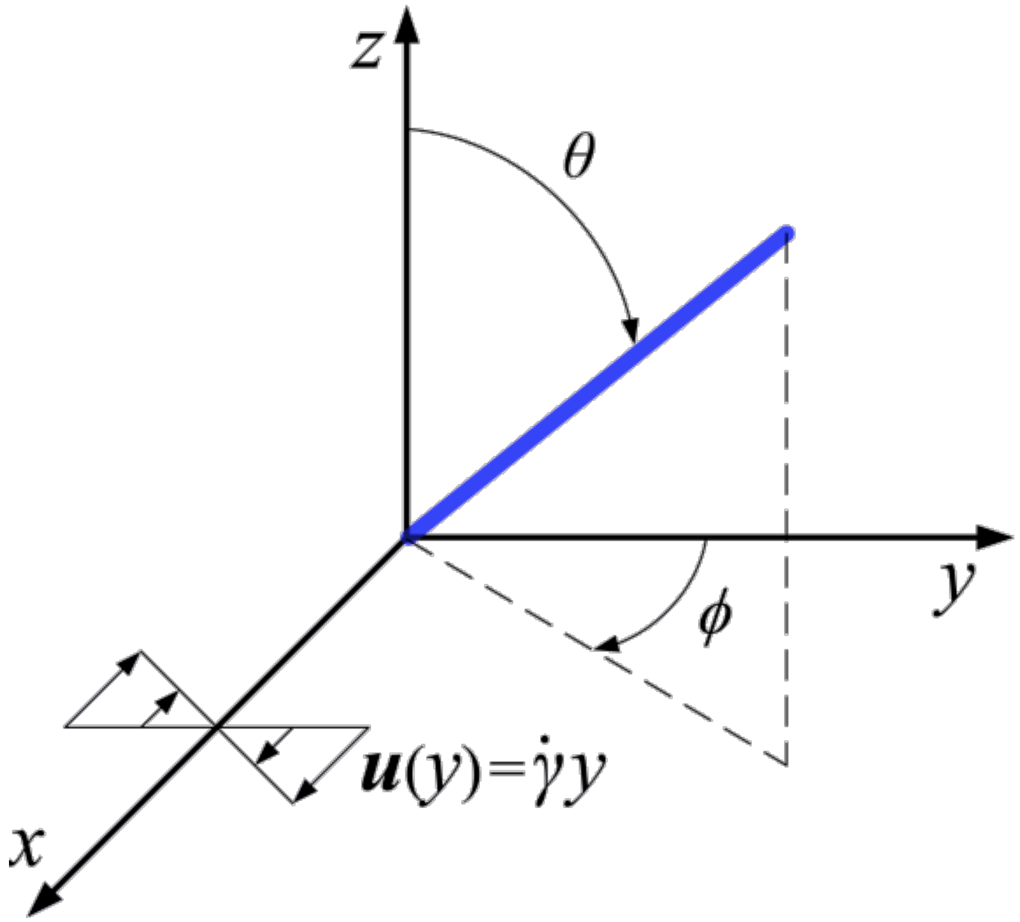

$$N_1 = \sum_{xx} - \sum_{yy}$$

Batchelor's relation: N_1

The stress in dilute suspension

$$N_1^B = \boldsymbol{\sigma}_{xx}^B - \boldsymbol{\sigma}_{yy}^B = \mu_{fiber}\dot{\gamma}\left(\left\langle \boldsymbol{p}_x^3 \boldsymbol{p}_y \right\rangle - \left\langle \boldsymbol{p}_y^3 \boldsymbol{p}_x \right\rangle\right) = -\frac{\mu_{fiber}\dot{\gamma}}{4}\left(\left\langle \sin^4\theta \sin 4\phi \right\rangle\right)$$

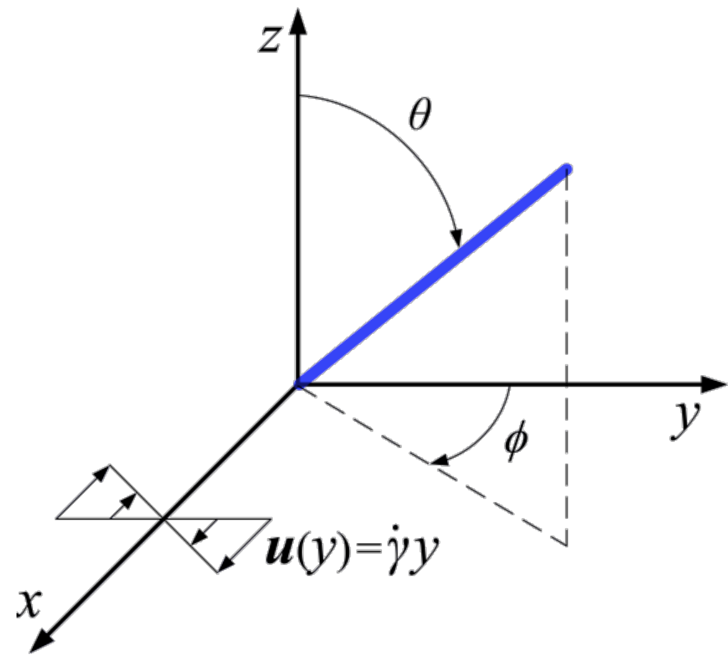

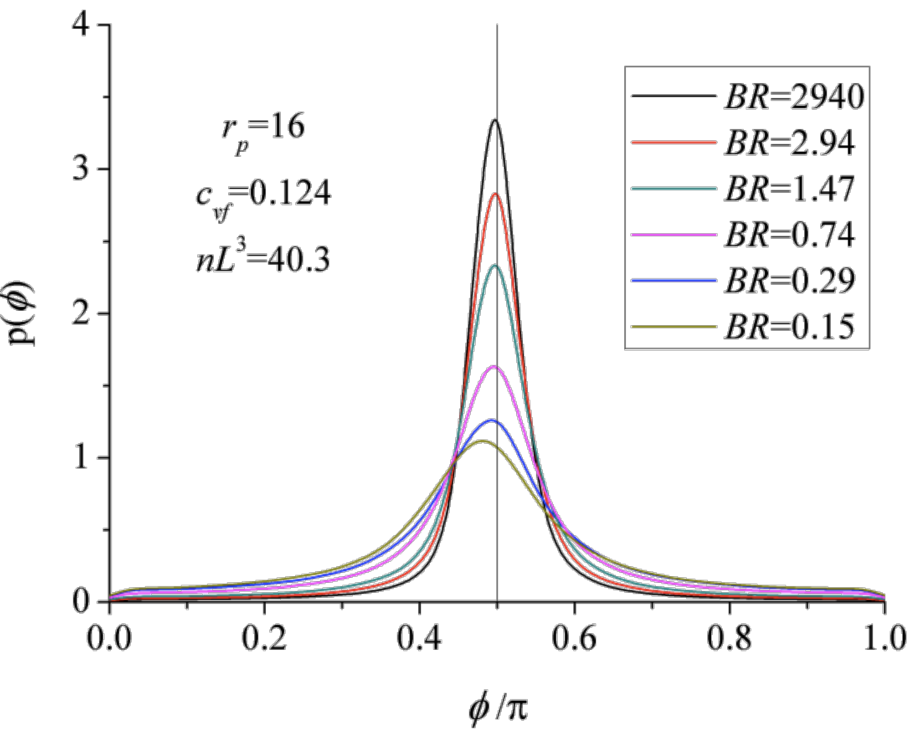

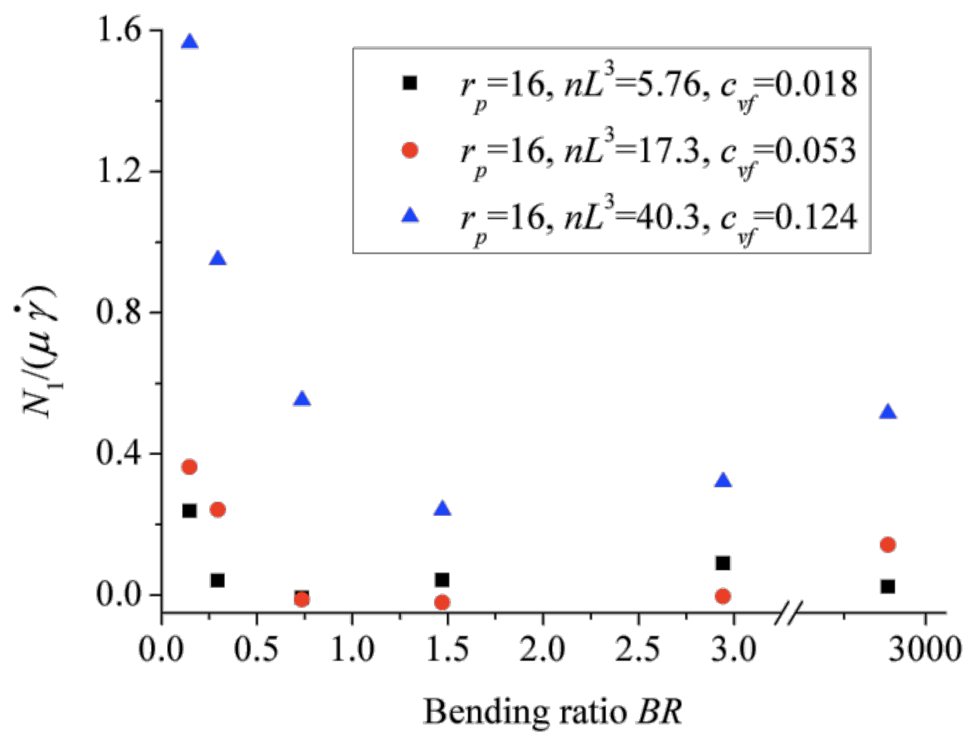

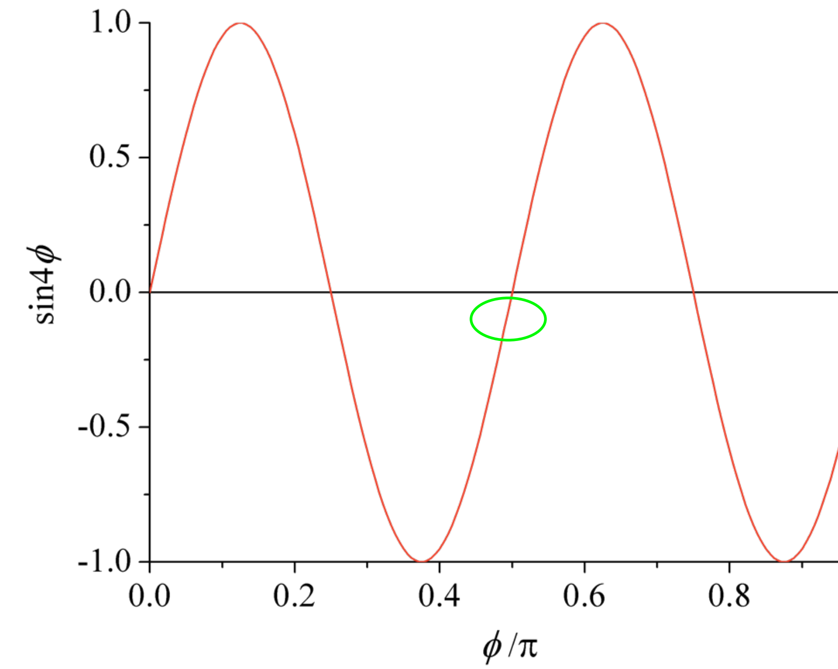

Batchelor, JFM, 1970

Batchelor's relation: N_1

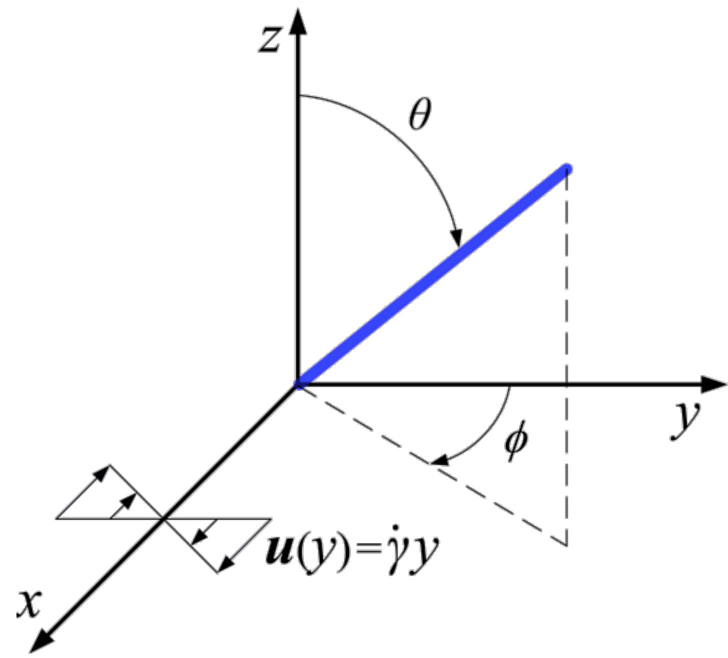

The stress in dilute suspensions

$$\boldsymbol{\sigma}^B = 2\mu\boldsymbol{E} + \mu_{fiber}\left(\langle \boldsymbol{pppp}\rangle - \frac{1}{3}\boldsymbol{I}_n\langle \boldsymbol{pp}\rangle\right):\boldsymbol{E}$$

$$N_1^B = \boldsymbol{\sigma}_{xx}^B - \boldsymbol{\sigma}_{yy}^B = \mu_{fiber}\dot{\gamma}\left(\langle \boldsymbol{p}_x^3\boldsymbol{p}_y\rangle - \langle \boldsymbol{p}_y^3\boldsymbol{p}_x\rangle\right) = -\frac{\mu_{fiber}\dot{\gamma}}{4}\left(\langle \sin^4\theta\sin 4\phi\rangle\right)$$

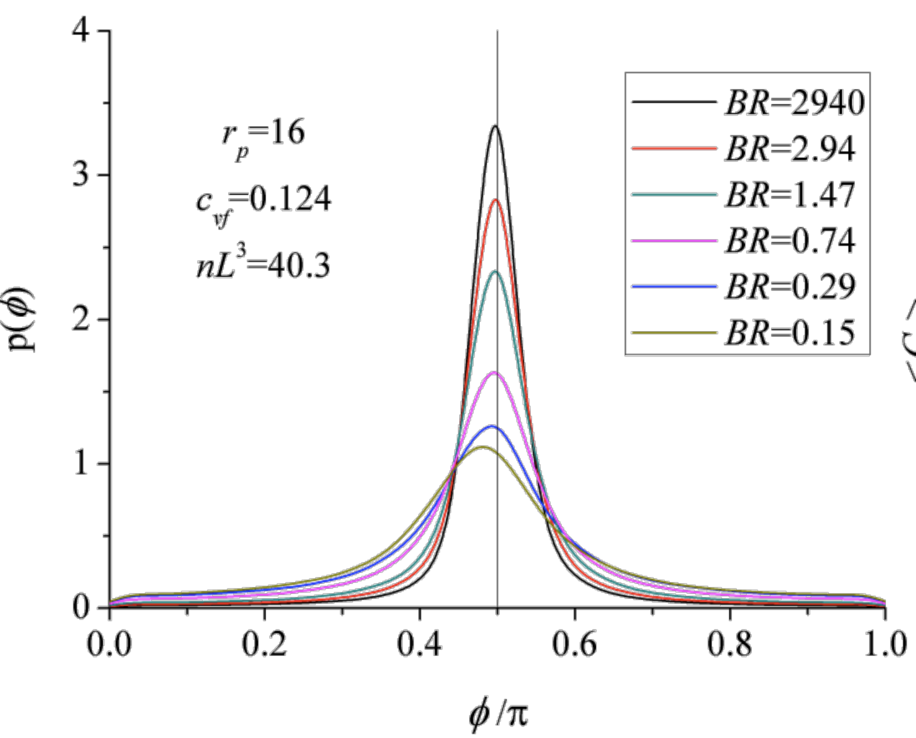

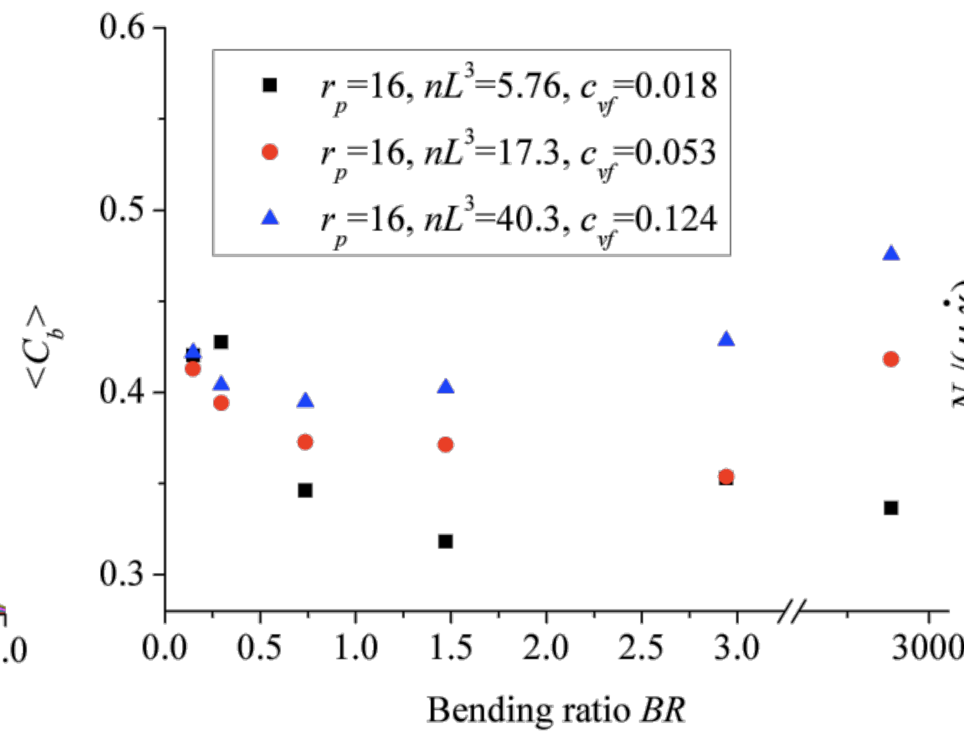

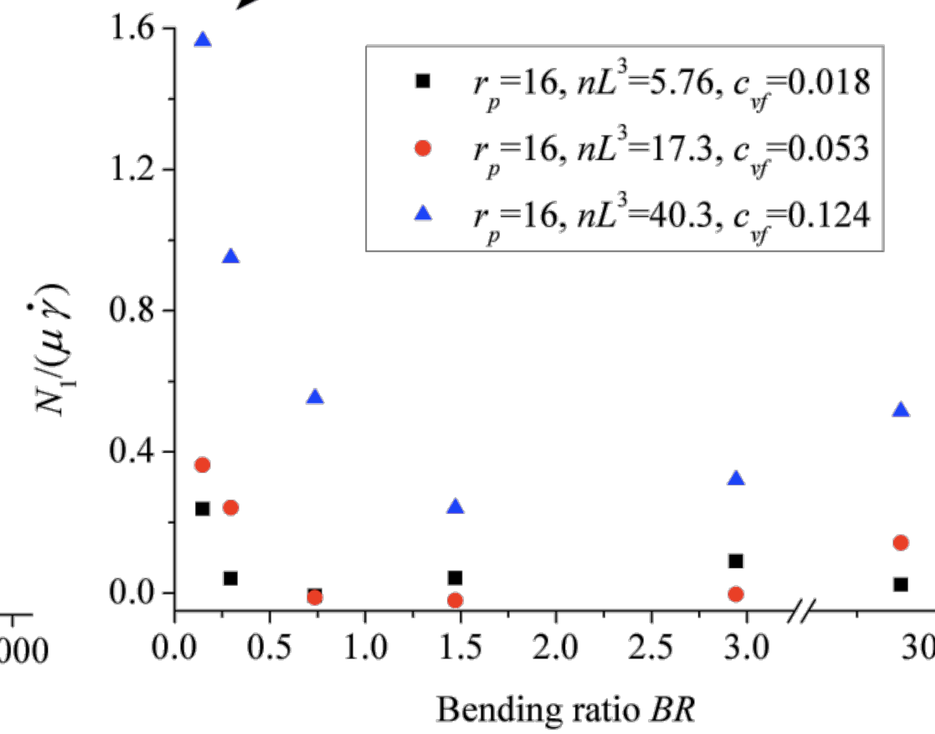

$$\tan\theta = \frac{C_j r_e}{\left(r_e^2\cos^2\phi + \sin^2\phi\right)^{1/2}}$$

$$C_b \equiv C_j/(C_j+1)$$

Batchelor, JFM, 1970

Relative Viscosity vs Shear rate

$AR = 16$
$c_{vf} = 0.0529$
$D = 0.12\text{mm}$
$\mu = 13$ Pa-s

$$\mathrm{Re} = \frac{\dot{\gamma} L D}{\nu}$$

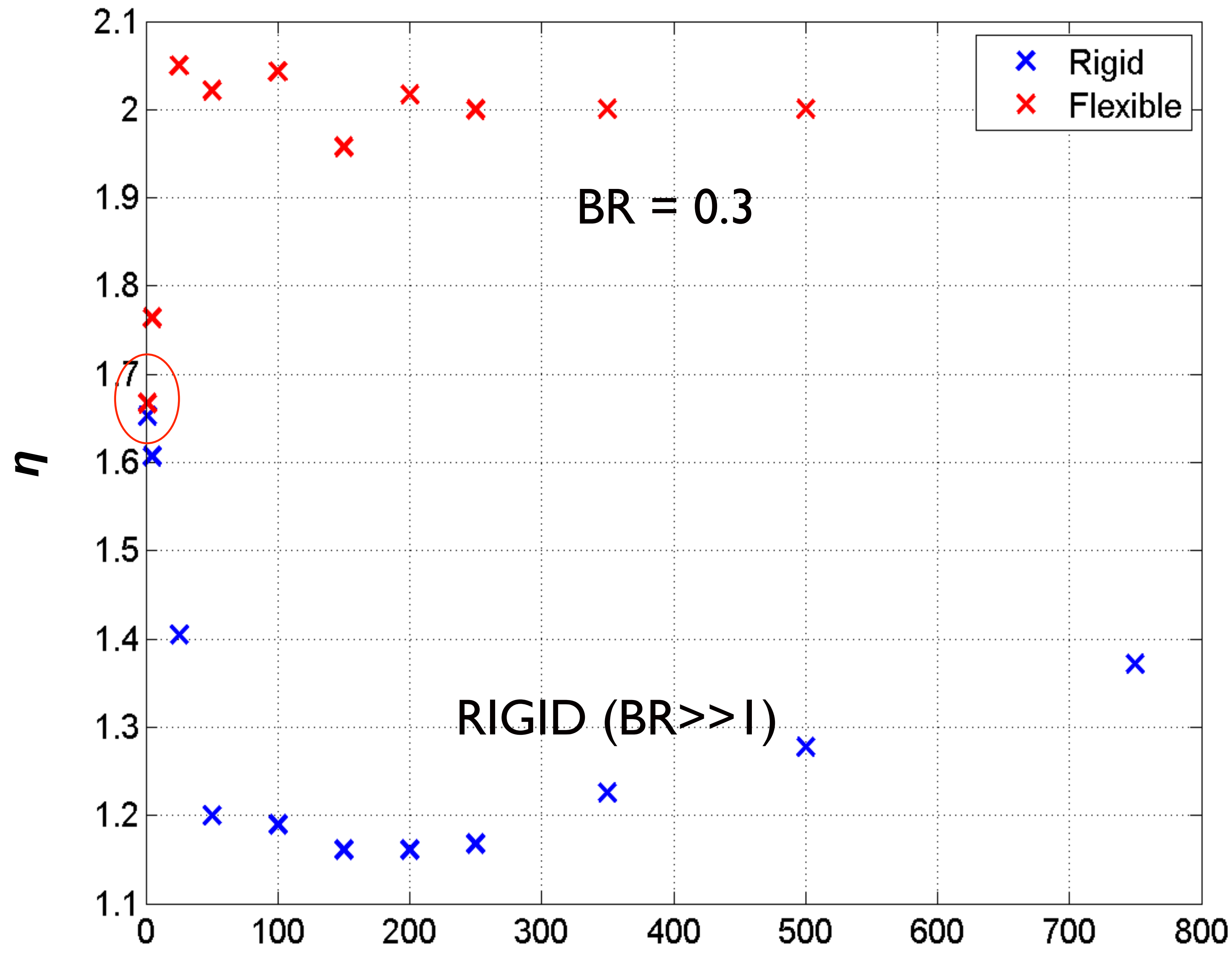

(Re~10^{-5}) **Shear rate (1/s)** (Re~10^{-2})

Conclusions

Relative viscosity increases as Bending Ratio decreases. This is due to broader fiber distribution, that is more fibers orienting in the compression and extension axes,

The primary normal stress difference seems to first decrease from stiff to slightly deformable fibers, and then increase sharply for highly deformable fibers. Orientation distribution is dominant….fiber-fiber contact less significant,

It appears that <u>fiber deformation</u> is the dominant factor in orientation distribution and relative viscosity as shear rate increases above 10, in the cases considered here;

Relative viscosity seems to be independent of shear rate for constant Bending Ratio

Wu and Aidun, *J. Fluid Mech.*, **662**, 122-33, 2010

Mubashar *et al.*, in preparation, ….